# Structural and energetic heterogeneity in protein folding. I. Theory

Steven S. Plotkin[a] and José N. Onuchic
*Department of Physics, University of California, San Diego, California*

(Received 8 September 2000; accepted 17 December 2001)

A general theoretical framework is developed using free-energy functional methods to understand the effects of heterogeneity in the folding of a well-designed protein. Native energetic heterogeneity arising from nonuniformity in native stabilizing interactions, as well as entropic heterogeneity intrinsic to the topology of the native structure, are both investigated as to their impact on the folding free-energy landscape and resulting folding mechanism. Given a minimally frustrated protein, both structural and energetic heterogeneity lower the thermodynamic barrier to folding. When energy functions consist of pair interactions, designing in sufficient heterogeneity can eliminate the barrier at the folding transition temperature. Sequences with different distributions of native stabilizing interactions and correspondingly different folding mechanisms may still be good folders to the same structure. This theoretical framework allows for a systematic study of the coupled effects of energetics and topology in protein folding, and provides interpretations and predictions for future experiments which may investigate these effects. © *2002 American Institute of Physics.* [DOI: 10.1063/1.1449866]

## I. INTRODUCTION

Theories of protein folding currently focus primarily on predicting properties of the folding mechanism given that the native structure and/or energy function is known *a priori*. One of the most powerful approaches to this end has been the energy landscape theory, used in one form or another in most descriptions of folding.[1–15] This approach takes advantage of the huge number of conformational states available to a protein by treating the energetics of those conformations statistically, just as the description of a phase transition from a liquid to a crystal is understood through the application of statistical mechanics to the numerous degrees of freedom in the problem. However, in understanding the self-organization of proteins and biological systems in general, it is necessary to study properties particular to finite-sized systems, e.g., barrier heights and corresponding rates. For a finite system such as a protein, characteristic features present in the amino acid sequence give rise to residual signatures in thermodynamic and kinetic properties. For example, although the four-helix proteins Im7 and Im9 are structural homologues, Im9 folds by a two-state mechanism while Im7 folds through an *en route* intermediate:[16] the free-energy landscape may fluctuate sequence to sequence for a chains that fold to the same native structure. Other experiments also indicate that rates and/or intermediates may differ for structural homologues.[17,18]

Since a knowledge of the native structure alone does not completely determine the free-energy profile, we might ask what information does, and also what parameters must be known to predict other properties of the folding mechanism, such as the specificity or diffusivity of the folding nucleus, for example.[19–22] By analyzing the energetic statistics of ensembles of states, landscape theory provides a framework to distinguish folding processes common to an ensemble of sequences from those peculiar to individual sequences. A particular property, for example folding transition temperature $T_F$, is not strongly dependent on the detailed Hamiltonian of the protein, but only on a few thermodynamic parameters. The folding temperature may then be expected to be a universal or self-averaging property for the ensemble of sequences having these parameters. Because $T_F$ is found by equating the total free energy of the folded and unfolded states, it should be only weakly sensitive to the details of the actual distribution of native state stabilizing interactions within the protein. On the other hand, properties such as the folding barrier and its corresponding rate may depend strongly on the distribution of native stability throughout the protein, i.e., on the distribution of native stabilizing interactions.

To theoretically treat the thermodynamics of folding and unfolding, we quantify a model protein in terms of the full native Hamiltonian $\{\epsilon_i\}$, as well as the full distribution of native contact lengths $\{l_i\}$, under the assumption that the protein under consideration is well-designed, i.e., with its folding temperature $T_F$ larger than its glass temperature $T_G$. Here, $i$ is a single index which labels a native contact having loop length $l_i$ and energy $\epsilon_i$. Here, the overall native topology is characterized by the distribution $\{l_i\}$. Native heterogeneity is retained explicitly, while non-native interactions are treated through a scalar background field representing the average effects of non-native trapping.[23,24] We are thus isolating the effects of native heterogeneity on the folding mechanism.

The formalism we develop here allows us to treat both the energetics and the entropics involved in folding. In the specific functional we derive, the energetics enter straightforwardly, and a mean-field approximation is made to treat the

[a]Current address: Department of Physics and Astronomy, University of British Columbia, 6224 Agricultural Road, Vancouver, BC V6T 1Z1, Canada. Electronic mail: steve@physics.ubc.ca

 

entropics. Other treatments for the entropics are of course possible within the general framework we develop, e.g., a spatially contiguous or capillarity nucleus,[25,26] or even an exact entropy functional obtained from enumeration of states.

Certainly, if the entropy around the transition state were small, as occurs when a protein is not well-designed, the position and height of the rate determining barrier(s) would fluctuate wildly from sequence to sequence. However, since proteins have evolved native stabilities larger than their rms non-native energy scale,[2,27–33] the temperature $T_F$ where the native state is stable is sufficiently higher than $T_G$, so there is an extensive amount of entropy in the transition state under folding conditions (e.g., see Fig. 7). Nevertheless, we find that even though there is a large entropy present in the system, there are still in fact strong dependencies of the barrier and folding mechanism on the distribution of native stabilizing interactions and distribution of native contact lengths. In fact, fluctuations in the native stabilizing interactions as well as in native contact lengths do not average out, but contribute extensively in determining properties of the folding mechanism![34]

If a property is not self-averaging over a given ensemble of sequences, the parameters specified to determine the ensemble are either not sufficiently accurate or are incomplete. For example, the folding transition temperature $T_F$ is not self-averaging over the ensemble of sequences that fold to a particular native structure, since these different sequences may have different native stability, flexibility, etc. Nonetheless, a quantity such as folding temperature or folding barrier which fluctuates over an incompletely specified ensemble may have a mean that is still useful in characterizing trends as a function of one or more parameters. An example is the increase on average in folding rate, or decrease in folding barrier, as mean native contact length $\overline{l}$ (more specifically, $\overline{l}/N$) is decreased,[35] for which several models have been proposed,[36,37] and which we consider here within our theoretical framework as well (see section IV C). The observed correlation between rates and $\overline{l}$ implies that many proteins are sufficiently well-designed such that native topology plays an important if not dominant role in governing folding mechanism, a topic recently investigated by several authors.[36–48] That is, if these proteins were poorly designed, folding rates would strongly fluctuate sequence to sequence, even for sequences with the same ground state structure.

Our intention here is to go beyond the first moment of the contact length distribution $\overline{l}$ or stability distribution $\overline{\epsilon}$. We investigate how the full distributions of energetics and topology as well as correlations between them affects the free-energy profile, corresponding barrier, folding rate, and overall folding mechanism. Expanding on our previous work,[49] we find that native heterogeneity, both entropic and energetic, plays an important role in quantifying protein folding mechanisms. We show how one can extend the analysis of thermodynamic quantities by using functionals to describe folding properties which are not necessarily self-averaging but which may depend on distributions of coupling parameters. To this end we derive a simple field theory with a nonuniform order parameter to study fluctuations away from uniform ordering, through free-energy functional methods introduced earlier by Wolynes and collaborators.[39,50,51] The theory is in good agreement with simulations of model proteins.[49,52] Similar effects have also been observed in Monte Carlo simulations of sequence evolution for lattice protein models, when the selection criteria involves fast folding rate.[53] Here we see how, from general considerations of the energy landscape theory, selecting for rate can induce heterogeneity in the participation of contacts which make up the transition state ensemble. The folding barrier for a well-designed protein is maximized when the nucleus is the most diffuse. This minimizes conformational fluctuations around the native state. For typical values of native energies, well-designed proteins have funneled folding mechanisms with heterogeneous native contact participations.[54–58]

Our results are also supported by several experiments in the literature as described in the Conclusions section, and suggest experiments to be performed. For example, the reduction of barrier height with folding heterogeneity (a folding mechanism with preferred folding routes) should be experimentally testable by measuring the dependence of folding rate for a well-designed protein on the dispersion of $\phi$ values,[59] as might be obtained from structural homologues or circular permutants. It is important that before and after the mutation(s) the protein remains fast-folding, preferably a two-state folder, to the native structure without ''off-pathway'' intermediates, and that its native state stability remain approximately the same, perhaps by tuning environmental variables.

In the arguments below we associate reductions in the free-energy barrier $\Delta F^{\ddagger}$ to increases in the folding rate $k_F$. This is true as long as the prefactor $k_0$ in the expression for the rate

$$k_F = k_o e^{-\Delta F^{\ddagger}/T}, \tag{1.1}$$

is more weakly affected than the barrier height under redistribution of native stabilizing interactions. While the distribution of native stabilizing interactions must indeed couple with the specific distribution of non-native interactions, for well-designed proteins with large transition-state entropy, it is more likely that the effect on the prefactor comes from the coupling of the folding transition temperature $T_F$ to the distribution of native stabilizing interactions, as long as the protein still folds to the same native structure. In other words we must consider the effect on the prefactor as the ratio of the transition temperature to glass temperature $T_F/T_G$ changes, or as the protein becomes more strongly well-designed or less well-designed. However, it has been shown[49,52] that there is a range of heterogeneity and corresponding folding mechanism where $T_F/T_G$ is approximately constant, while the barrier height varies significantly. As long as the contact energies follow a range of parameters such that the global properties of the folding funnel do not change, i.e., $T_F/T_G$ varying slowly and sufficiently larger than 1, lowering the free-energy barrier is essentially equivalent to increasing the rate. However, one has to be careful that the folding heterogeneity is not so large that this regime breaks down. We focus here on this funneled regime, where the barrier height

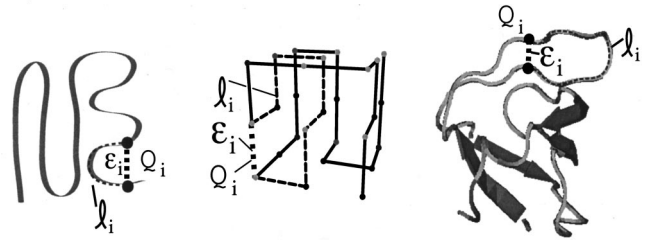


FIG. 1. Schematic, lattice, and off-lattice representations of the native structure, characterized through the distribution of contact energies $\{\epsilon_i\}$ and contact entropies $\{s_i\}$, (defined through the distribution of loop lengths $\{l_i\}$). The probability to form contact $i$ having energy $\epsilon_i$ and loop length $l_i$ is $Q_i$.

is the strongest determinant of the folding rate. It can be shown[52] that for Gō-type models with native interactions alone,[60–62] the distribution of native contact energies does not strongly affect the reconfiguration kinetics appearing in the prefactor, compared to its effect on the barrier height.

When the Hamiltonians consists of pair interactions alone, redistributions of native stabilizing interactions can eliminate the barrier entirely at the folding temperature. It is worth noting that many-body interactions which are believed to be present in real protein interactions[63–69] tend to increase the barrier height,[24,70,71] and in their presence the barrier may be more robust to redispersement of native stabilizing interactions.

A funnel folding mechanism consisting of a large number of routes to the native structure is preserved for a wide variety of folding scenarios and barrier heights, including folding through on-pathway intermediates. For the distributions of native energy necessary to induce folding through one or a few routes, the folding temperature drops by about a factor of 6,[49] which indicates that for realistic energy functions which are also composed of non-native interactions, folding would be exceedingly slow at the low temperatures where the native state would be stable. However, for proteins which are large and multidomain, it is possible that entropic or energetic heterogeneity may induce significantly route-like folding near typical folding conditions.

This paper is organized as follows: First, we outline the general strategy of the calculation in Sec. II. The free-energy functional is then derived in Sec. III, and the general effects of heterogeneity in folding are investigated for this functional in Sec. IV. Finally, we conclude and suggest future research.

## II. THE GENERAL STRATEGY

It is first necessary to characterize the generic properties of the native state. We adopt a coarse-grained description for the native structure, and describe it by its distributions of native contact energies $\{\epsilon_i\}$ and native loop lengths or contact lengths $\{l_i\}$ (see Fig. 1). Here, $\epsilon_i$ is the solvent averaged effective energy of contact $i$, and $l_i$ is the sequence length pinched off by contact $i$ (see Fig. 1).[72] We use a single subscript for the labeling index $i$ because we are only considering effects on the particular set of native contacts for a given native structure. Non-native interactions are treated by an average field, since the protein is assumed to be well-designed to its native structure, and native interactions are then most important in determining the folding mechanism. The index $i$ runs from 1 to $M$, where $M$ is the number of residue pair contacts in the lowest energy native structure. $M$ scales roughly extensively, i.e., $M=zN$, with $N$ the number of residues in the polymer chain. Here, $z$ is the mean number of contacts per residue: a function of either the lattice coordination number or the off-lattice cutoff length. It is of order 1, with surface area corrections dying away as $N^{-1/3}$.[73] We can quantify nativeness in the first approximation by the fraction of native contacts $Q$, with $0<Q<1$. Other parameters are also reasonable for stratifying the landscape: the fraction of correct (native) dihedral angles,[31] coarse-grained position in space in the native structure,[23,74] or even the ensembles having a given probability to fold before unfolding.[75] But, $Q$ is the most suitable for calculation in the present theory. At partial degrees of nativeness the probability to form contact $i$ is defined as $Q_i(Q)$, and we define $Q_i^*(Q)$ as the fraction of time contact $i$ is formed at equilibrium in the ensemble with $MQ$ native contacts, or equivalently the fraction of proteins in a macroscopic sample with a given degree of nativeness having that contact formed. Nonuniformity in $Q_i^*$ values at partial degrees of nativeness would indicate that the protein prefers to fold some regions over others. The distribution $\{Q_i(Q)\}$ for all $Q$ is a measure of the folding mechanism for the protein under consideration.

Following the formalism used in inhomogeneous fluids[76,77] and the theory of first-order transitions,[78] we write a free-energy functional $F(\{Q_i\},\{\epsilon_i\},\{l_i\})$ to characterize the effects of structural and energetic heterogeneity superimposed on the overall folding funnel. This approach has been used previously by Bohr and Wolynes to describe domain growth in proteins[79] and more recently as a calculational tool for experimental $\phi$ values.[39,50,51]

The free-energy functional is first interpreted as depending upon the local contact probabilities $Q_i(Q)=\langle\Theta(r_i-r_i^{\mathrm{N}})\rangle_{\mathrm{T}}(Q)$, where $i$ labels the native contact between two residues, $r_i$ the distance between them, $\Theta$ is a function that measures proximity such as a step function for off-lattice models or a Kronecker delta for nonbonded nearest neighbor sites on-lattice, and $\langle\cdots\rangle_{\mathrm{T}}$ indicates an average over the ensemble at $Q$. We will typically take $\langle\cdots\rangle_{\mathrm{T}}$ to be a Boltzmann-weighted average; then, $Q_i^*$ is the thermally averaged fraction of the time two parts of the protein are in proximity (contact)[80]

$$Q_i^*(Q)=\langle\delta_i\rangle_{\mathrm{T}}=\sum_{c\in Q}{}'\,\delta(i,c)\,\frac{\exp(-E_c/T)}{Z(Q)}, \tag{2.1}$$

where $\delta(i,c)=1$ if contact $i$ is made in configuration $c$, and $\delta(i,c)=0$ otherwise, and $Z(Q)=\Sigma'_{c\in Q}\exp(-E_c/T)$ is the partition function for the configurations at $Q$. The sum may be taken over any ensemble of theoretical interest. Here, we have in mind the ensemble defined as having a given degree of overall order $Q=(1/M)\Sigma_i Q_i$.[81]

In the functional method, all the contact energies $\{\epsilon_i\}$ and loop lengths $\{l_i\}$ for a protein are initially assumed as given, and a free-energy functional $F(\{Q_i(Q)\}|\{\epsilon_i\},\{l_i\})$ is

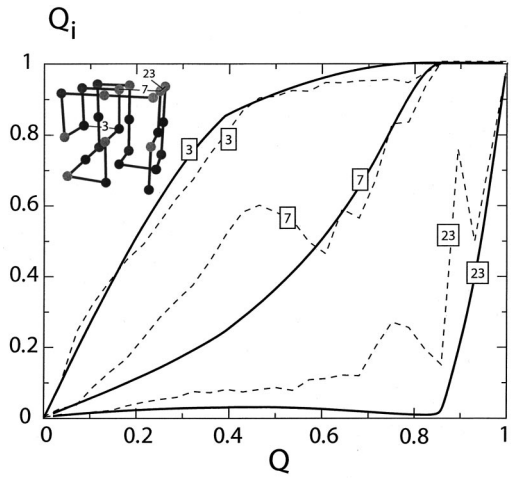


FIG. 2. The fraction of time or probability $Q_i^*(Q)$ that a contact is made as a function of $Q$, for folding to the lattice structure shown in Fig. 1. Solid curves are the result of the functional theory of Sec. III, and dashed curves are Monte Carlo simulation results for folding to this structure (Refs. 49, 52). Short-ranged contacts tend to be formed earlier than long-ranged contacts. Shown here are a representative contact for the loop lengths $l_i = 3,7,23$. The contacts are indicated by thin solid lines on the lattice model native structure in the upper left. Note that occasionally nonmonotonic $Q$ dependence is observed in the simulations. Also, some short-ranged contacts near the protein surface remain only partially formed until large degrees of nativeness.

derived in terms of a general (arbitrary) distribution of contact probabilities $\{Q_i(Q)\}$. The thermal (most probable) distribution of contact probabilities $\{Q_i^*(\{\epsilon_i\},\{l_i\},Q)\}$ is found by minimizing the free-energy functional $F(\{Q_i(Q)\}|\{\epsilon_i\},\{l_i\})$ with respect to the distribution of contact probabilities, subject to the constraint that the average probability is $Q$, i.e., $\Sigma_i Q_i = MQ$ ($Q$ then parametrizes the values of the $Q_i's$). Examples of the functions $Q_i^*(Q)$ are plotted in Fig. 2. This procedure is analogous to finding the most probable distribution of occupation numbers, and thus the thermodynamics, by maximizing the microcanonical entropy for a system of particles obeying a given occupation statistics. Here, the effective particles (the contacts) obey Fermi–Dirac statistics [see Eq. (3.34)], since no more than one bond can ''occupy'' a contact. The system can be understood to have a set of free-energy levels obeying a distribution governed by the native structure and energies of the protein, and we seek the fraction of time (the probability) those levels are occupied given a fixed overall number of levels filled.

The free energy for a system obeying the thermal (most probable) distribution $\{Q_i^*(Q,\{\epsilon_i\},\{l_i\})\}$ is then considered a function of the contact energies for a *fixed* native structure: $F(Q,\{\epsilon_i\}|\{l_i\})$. That is, we consider the folding free-energy barrier as a functional of the interaction energies $\{\epsilon_i\}$ for a *given* native topology. The free energy depends on the energies $\{\epsilon_i\}$ both explicitly and implicitly through the thermal contact probabilities $\{Q_i^*(\{\epsilon_i\}|Q,\{l_i\})\}$. Then, we can seek the special distribution of contact energies $\{\epsilon_i^*(l_i)\}$ that extremizes (minimizes or maximizes, depending on the second derivative) the thermodynamic folding barrier to a particular structure by finding the extremum of $F^\dagger(\{\epsilon_i\}|\{l_i\})$ with respect to the contact energies $\epsilon_i$, subject to the constraint of fixed total native energy: $\Sigma_i \epsilon_i = M\overline{\epsilon} = E_N$, i.e., while maintaining the same overall stability of the native structure. Thus, we are isolating the effect of heterogeneity on the folding mechanism. This distribution, when substituted into the free energy, gives in principle the extremum free-energy barrier as a function of native structure $F^\dagger(\{l_i\})$, which might then be optimized for the fastest/slowest folding structure and its corresponding barrier. However, we found that the only distribution of energies for which the free energy was an extremum is in fact the distribution which *maximizes* the barrier by tuning all the contact probabilities to the same value: $Q_i(Q^\dagger) = Q^\dagger$. In this case the coupling energies would be tuned to eliminate any information contained in the native structure, except for the mean loop length $\overline{l} = (1/M)\Sigma_i l_i$. Any perturbation away from this scenario lowers the free-energy barrier. We also examine the effects of structural dispersion on the barrier, i.e., a free energy for variable loop distribution but fixed coupling energies $F(Q,\{l_i\}|\{\epsilon_i\})$, and arrive at the same conclusion: for fixed energies, increasing structural variance (at fixed average loop length) lowers the barrier and thus speeds the rate, as long as the proteins are sufficiently well-designed that the rate is governed by the free-energy barrier.

## III. FREE-ENERGY FUNCTIONAL

In this section we derive the free-energy functional to be used in the main analysis. We first show how the functional is related to the Hamiltonian. Then in section III B the entropic terms present in the functional are derived. In III D the thermal contact probabilities are obtained by minimizing the free-energy functional.

### A. Obtaining the functional from a Hamiltonian

We can motivate the form of the free-energy functional from landscape arguments, i.e., by considering energy distributions of states with structural similarity to the native. Consider a contact Hamiltonian $\mathcal{H}$ of the form

$$\mathcal{H}(\{\Delta_{\alpha\beta}\}|\{\Delta^N_{\alpha\beta}\}) = \sum_{\alpha<\beta} [\epsilon^N_{\alpha\beta}\Delta_{\alpha\beta}\Delta^N_{\alpha\beta} + \epsilon_{\alpha\beta}\Delta_{\alpha\beta}(1-\Delta^N_{\alpha\beta})], \tag{3.1}$$

which gives the energy of a particular configuration defined by the set of contact interactions $\{\Delta_{\alpha\beta}\}$. This Hamiltonian gives energy $\epsilon^N_{\alpha\beta}$ to the contacts which are native contacts, and energy $\epsilon_{\alpha\beta}$ to non-native contacts. We embody the principle of minimum frustration[27] by making the mean of the distributions from which native contact energies are chosen be lower than the mean of the distribution for non-native contact energies. Native contacts may also have a smaller variance, depending on the effective number of letters in the sequence. For example, simplified models consisting of only two types of residues ''H'' and ''P'' (2-letter codes) have a $2\times2$ matrix of pair interaction energies, and tend to have nearly all H–H contacts in the ground state, resulting in nearly zero variance in the native stabilizing energies. The energies in (3.1) are internal free energies of spatially short-ranged interaction between effective monomeric units, after averaging over side chain and solvent degrees of freedom.

The double sum is over residue indices, and $\Delta_{\alpha\beta}=1$ if residues $\alpha$ and $\beta$ are in contact in a configuration; $\Delta_{\alpha\beta}=0$ otherwise. $\Delta^{\mathrm{N}}_{\alpha\beta}=1$ if these residues are also in contact in the *native* configuration, and $\Delta^{\mathrm{N}}_{\alpha\beta}=0$ otherwise. $\epsilon^{\mathrm{N}}_{\alpha\beta}$ and $\epsilon_{\alpha\beta}$ are again the energies of native and non-native contacts, respectively.

We obtain the thermodynamics for this system by considering statistical properties of an ensemble of partially native states. Once the density of states $n(E|\{Q_i\})$ is known, the thermodynamics at temperature $T$ can be obtained. We obtain a statistical average of $n(E|\{Q_i\})$ from a knowledge of the overall number of partially native states, and the probability each of these states has a given energy. A similar derivation for a homogeneous order parameter $Q$ was calculated in Ref. 24. The probability a configuration with a particular set of native contacts $\{\Delta_{\alpha\beta}\Delta^{\mathrm{N}}_{\alpha\beta}\}$ has energy $E$ is given by

$$P(E\{\Delta_{\alpha\beta}\Delta^{\mathrm{N}}_{\alpha\beta}\})=\langle\delta[E-\mathcal{H}\{\Delta_{\alpha\beta}\}]\rangle_{\text{non-nat}} \tag{3.2}$$

where the averaging is over the non-native contact coupling energies

$$\langle\cdots\rangle_{\text{non-nat}}=\int\prod_{\text{non-nat}}P(\epsilon_{\alpha\beta})d\epsilon_{\alpha\beta}.$$

Residual features in the folding mechanism may be present due to non-self-averaging effects of non-native interactions, resulting in phenomena such as ''off-pathway'' intermediates. We preclude the existence of any distinct non-native traps with the above procedure, and consider only an average non-native background field, while native interactions are explicitly retained. This is a formal way of asserting that native interactions are more important than non-native interactions in determining rates and mechanisms for a minimally frustrated heteropolymer. Thus, ''on-pathway'' intermediates, or fluctuations in the free-energy landscape due to native structural or energetic heterogeneity are retained in this procedure. Averaging the Fourier-transformed delta function over non-native interactions chosen from a Gaussian distribution

$$P(\epsilon_{\alpha\beta})=\frac{1}{(2\pi b^2)^{1/2}}\exp\left(-\frac{(\epsilon_{\alpha\beta}-\overline{\epsilon}_{nn})^2}{2b^2}\right),$$

results in

$$P(E\{\Delta_{\alpha\beta}\Delta^{\mathrm{N}}_{\alpha\beta}\})=\frac{1}{[2\pi Mcb^2(1-Q)]^{1/2}}\times\exp\left(-\frac{(E-\overline{E}-\Sigma_i\epsilon_iQ_i)^2}{2Mcb^2(1-Q)}\right), \tag{3.3}$$

where $\overline{E}=Mc\overline{\epsilon}_{nn}$ with $c$ the packing fraction $(0<c<1)$, and where the sum over native contacts $\Sigma_{\alpha\beta}\epsilon^{\mathrm{N}}_{\alpha\beta}\Delta_{\alpha\beta}\Delta^{\mathrm{N}}_{\alpha\beta}$ is written in the shorthand single index notation $\Sigma_i\epsilon_iQ_i$, i.e., $Q_i\equiv\Delta_{\alpha\beta}\Delta^{\mathrm{N}}_{\alpha\beta}$. Here, $Q_i=0$, 1 but in the free-energy functional, fractional values are allowed. We will see that the thermal values of the contact probabilities $Q_i^*=\langle\Delta_{\alpha\beta}\Delta^{\mathrm{N}}_{\alpha\beta}\rangle_{\mathrm{T}}$ are the fractional values that minimize the functional [cf. Eq. (3.34)].

When the number of states $n(E|\{Q_i\})$ is large, it can be replaced by the disorder-averaged number $\Omega(\{Q_i\})P(E|E_{\mathrm{N}},\{Q_i\})$, since the relative fluctuations in the number die away as $M^{-1/2}$ for uncorrelated disorder. Then,

$$\log n(E|\{Q_i\})\approx S(\{Q_i\})-\frac{(E-\overline{E}-\Sigma_i\epsilon_iQ_i)^2}{2Mcb^2(1-Q)}. \tag{3.4}$$

The term $S(\{Q_i\})$ is the configurational entropy, discussed below. The thermal energy $E(T|\{Q_i\})$ is obtained from the density of states above through $\partial\log n(E)/\partial E=T^{-1}$

$$E(T|\{Q_i\})=\overline{E}+\sum_i\epsilon_iQ_i-\frac{Mcb^2}{T}(1-Q). \tag{3.5}$$

This procedure is applicable in the high-temperature regime when the number of states occupied at such temperatures is large. The energy consists of an integration over an energy density, i.e., by an energy per contact times the probability that contact is made, $\epsilon_iQ_i$, summed over all contacts, minus a term corresponding to a lowering of the thermal energy due to the net effect of non-native traps. We ignore any coupling of non-native packing fraction with nativeness; since this subtle effect only enters in here at the mean-field level and we are focusing on heterogeneity effects, we treat $\overline{E}$ as a constant.[82]

Substituting (3.5) into (3.4) gives the thermal entropy

$$S(T|\{Q_i\})=S(\{Q_i\})-\frac{Mcb^2}{2T^2}(1-Q), \tag{3.6}$$

which consists of the entropy of the polymer chain subject to the geometric constraints $\{Q_i\}$ of contact formation, $S(\{Q_i\})$, and a lowering term due to the presence of non-native traps (fluctuations in Boltzmann weights due to the fluctuations in state energies reduces the effective total number of states occupied). The temperature dependence of $S(\{Q_i\})$ appears through the implicit temperature dependence of the contact probabilities $Q_i$ [see Eq. (3.34)].

At this point, since no exact solution for the entropy of a three-dimensional polymer containing topological constraints is known, we must either resort to an accurate solution for an approximate, idealized model system, or an approximate phenomenological treatment of the real system. We choose the latter approach for the theory, and the former approach in the simulations we performed.[49,52] While still an approximation, the entropy we derive captures many of the same quantitative effects we see in the simulations, which contain an accurate computation of the entropy for the idealized lattice model, to the extent that higher-order correlations between the formation of various contacts are implicitly accounted for. When computing the entropy in the contact representation, we must first calculate how much entropy the unconstrained polymer has, $Ns_o$. Then, we define the entropy that corresponds to the degeneracy of contact patterns having functional order $\{Q_i(Q)\}$ as $\mathcal{S}_{\mathrm{ROUTE}}(\{Q_i(Q)\})$ $(\mathcal{S}_{\mathrm{ROUTE}}>0)$, and the configurational entropy lost from the coil state to induce the ordering specified by $\{Q_i\}$ as $\mathcal{S}_{\mathrm{BOND}}(\{Q_i\}|\{l_i\})$ $(\mathcal{S}_{\mathrm{BOND}}<0)$. The total conformational entropy is then given by

$$S(\{Q_i\})=Ns_o+\mathcal{S}_{\mathrm{ROUTE}}(\{Q_i\})+\mathcal{S}_{\mathrm{BOND}}(\{Q_i\}|\{l_i\}). \tag{3.7}$$

These contributions are discussed below in Sec. III B.

The free-energy functional at temperature $T$ and nativeness $Q$ is written as $E-TS$ in terms of the field $\{Q_i\}$, using Eqs. (3.5), (3.6), and (3.7)

$$F(T|\{Q_i(Q)\}|\{\epsilon_i\},\{l_i\}) = \sum_i \epsilon_i Q_i - T\mathcal{S}_{\mathrm{ROUTE}}(\{Q_i\}) - T\mathcal{S}_{\mathrm{BOND}}(\{Q_i\}|\{l_i\}) + \bar{E} - NTs_o - \frac{Mcb^2}{2T}(1-Q). \quad (3.8)$$

The terms on the first line of Eq. (3.8) depend on the native density field $\{Q_i\}$, while the remaining terms depend only on the uniform "background field" $Q$, and are not central to the main analysis, which considers specifically the effects of native heterogeneity in structure and contact energy.[83]

The native stability gap is composed of a sum of two-body interaction energies between $M$ pairs of native residues. Cooperative contributions to the energy function[24,84] necessary for *de novo* prediction[84,85] and accurately representing barriers[24,71] are not studied here, since native stability is present *a priori* in the free energy of our model, and thus we focus specifically on the properties of already well-designed sequences to a given structure, for which cooperative effects should induce quantitative but not qualitative changes in the results presented here.

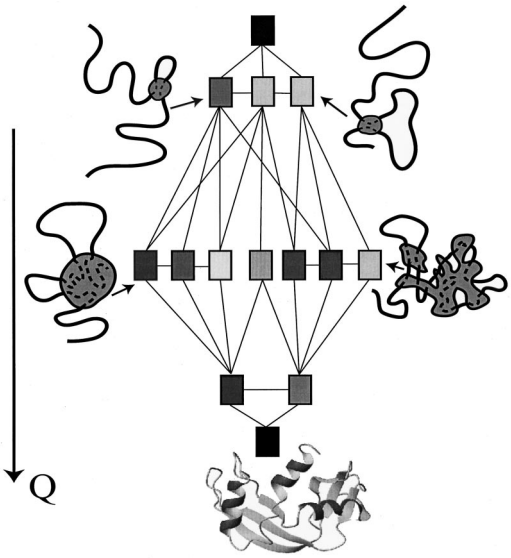


FIG. 3. Illustration of folding heterogeneity. At partial degrees of nativeness, a protein adopts conformations containing various native cores as indicated schematically (the core may be globular or ramified). These native cores are occupied with varying probabilities depending on their free energies (stronger probability is indicated here as a darker shade of gray). As folding heterogeneity increases, the entropy at degree of nativeness $Q$ decreases. However, the energy at $Q$ always decreases more, so that the free energy at $Q$ goes down. See also Ref. 118 for an illustration showing heterogeneity specifically for λ repressor within the diffusion–collision model.

### B. Entropic terms

If we imagine the ensemble of configurations that has a given amount of order, say a given number $MQ$ of native contacts, then within this ensemble there is a multiplicity of subensembles of states having different sets of $MQ$ contacts, whose thermal occupation we identify as a measure of the number of distinct routes in folding to the native state. Each subensemble contains many states corresponding to the entropy of the disordered polymer around the particular native core (e.g., see Fig. 3). We define the entropy that corresponds to the degeneracy of contact patterns having functional order $\{Q_i(Q)\}$ as $\mathcal{S}_{\mathrm{ROUTE}}(\{Q_i(Q)\})$ ($\mathcal{S}_{\mathrm{ROUTE}}>0$), and the configurational entropy lost from the coil state to induce the ordering specified by $\{Q_i\}$ as $\mathcal{S}_{\mathrm{BOND}}(\{Q_i\}|\{l_i\})$ ($\mathcal{S}_{\mathrm{BOND}}<0$).

#### 1. Route entropy

We make no capillarity or spinodal assumptions, and treat the route entropy $\mathcal{S}_{\mathrm{ROUTE}}(\{Q_i\})$ as a fairly simple modification of the entropy of a binary fluid mixture.[86] Binary fluid approximations to the route entropy in proteins, which scale extensively with system size, have been used previously.[24,39,50,51,79,87,88] The amount of route diversity in folding has also been analyzed in terms of the Shannon entropy,[89] which is similar in spirit to the following treatment.[49] The entropy of a binary fluid mixture is given through

$$\exp \mathcal{S}^o_{\mathrm{ROUTE}}(Q) = \frac{M!}{MQ!(M-MQ)!} \cong (\Omega^o)^M, \quad (3.9)$$

$$\Omega^o = Q^{-Q}(1-Q)^{-(1-Q)}, \quad (3.10)$$

which we interpret here as the product of $M$ factors of the number of states per contact at $Q$, $\Omega^o$ (e.g., at $Q=1/2$, $\Omega^o=2$), and is readily generalized to the case where the numbers of states per contact are not all equal: $\exp \mathcal{S}^o_{\mathrm{ROUTE}}(\{Q_i\}) = \Pi_{i=1}^M \Omega_i^o$, where $\Omega_i^o \equiv Q_i^{-Q_i}(1-Q_i)^{-(1-Q_i)}$. The principal modification introduced here for proteins is that, due to chain connectivity, as contact density increases, there is less sterically allowed space for a monomer to move around when one of its constraining contacts is broken. Thus, not all $M!/MQ!(M-MQ)!$ contact patterns have an entropy $\approx Ns_o + \mathcal{S}_{\mathrm{BOND}}$. In other words, making some native contacts forces spatially nearby contacts to be made because the corresponding monomers are forced to be in each other's proximity. So, there is a reduction from the putative number of states $(\Omega_i^o)^M$ since not all $M$ contacts are independently contributing to mixing, and several contact patterns correspond to the same constrained state. Here, we remove this degeneracy by dividing out the $(\Omega_i^o)^{M\zeta(\{Q_i\})}$ states that have been overcounted. Making a mean-field approximation for the local field around contact $i$ which reduces its number of states, $\Sigma_{\alpha\neq\beta} Q_{\alpha\beta}/\Sigma_{\alpha\neq\beta}(1) \simeq Q$, the new total number of states is $\Pi_{i=1}^M \Omega_i^{[1-\zeta(Q)]}$. Here, $\zeta(Q)$ is a monotonically increasing function of $Q$, from $\zeta(Q\to 0)=0$ to $\zeta(Q\to 1)=1$, since a nearly fully constrained polymer has all its entropy on the surface, making the mixing entropy per monomer negligible in the thermodynamic limit. We introduce the form $\zeta(Q)=Q^\alpha$, with $\alpha$ a parameter determined phenomenologically by a best fit to the lattice data, for example. Such a fit[49,52] yields $\alpha\approx 1$. The route entropy appearing in the free energy Eq. (3.8) then becomes

$$\mathcal{S}_{\rm ROUTE}(\{Q_i\}) = \log \prod_{i=1}^{M} \Omega_i^{\lambda(Q)}$$

$$= \lambda(Q) \sum_{i=1}^{M} [-Q_i \ln Q_i - (1-Q_i) \times \ln(1-Q_i)], \tag{3.11a}$$

$$\lambda(Q) \equiv 1 - Q^{\alpha}. \tag{3.11b}$$

The factor $\lambda(Q)$ measures the entropy reduction due to the coupling of chain connectivity with the native topology under study. The power $\alpha$ in $\lambda(Q)$ should be a decreasing function of the persistence length, and also of system size $N$, since for larger systems more polymer is buried and thus more strongly constrained by surrounding contacts. Variations in contact probabilities $Q_i$ will lower the route entropy [see Eq. (3.32)]. More detailed studies which treat the entropy loss due to chain connectivity are of course possible and are an interesting topic of future research.

### 2. Bond entropy

The calculation of the total entropy lost due to contact formation is rendered difficult because the entropy loss of a given contact depends not only on the contact's sequence length or bare loop length $l_i$, but also on the configuration of contacts $\{Q_i\}$ already present when the contact is formed. In spite of this difficulty some general statements can still be made, as follows.

If we make the assumption that the entropy loss to form contact $i$ depends explicitly only on the sequence length of contact $i$, as well as the full contact pattern present $\{Q_i\}$, then the most general form for the change in entropy due to contact formation, to go from configurations having one set of $Q_i$s parametrized in terms of a variable $t$, $\{Q_i(t_o)\}$, to another state having $\{Q_i(t_f)\}$, is

$$\mathcal{S}_{\rm BOND}(\{Q_i(t_f)\}|\{Q_i(t_o)\}) = \sum_i \int_{t_o}^{t_f} \mathcal{D}Q_i(t) s_i(l_i, \{Q_j(t)\}). \tag{3.12}$$

Here, $s_i(l_i, \{Q_j(t)\})$ is the entropy loss to form contact $i$ having sequence separation $l_i$, in the presence of the contact pattern $\{Q_j(t)\}$, which is itself parametrized through $t$.[90] Each $s_i(l_i, \{Q_j(t)\})$ in Eq. (3.12) is functionally integrated along the $M$-dimensional path specified by $\{Q_i(t)\}$. However, the entropy as a function of the set $\{Q_i\}$ must be a state function, meaning that the value of the integral depends only on the end points and not on the path taken. The condition for path independence is obtained as follows. We can envision a small subsection of the $M$-dimensional path as traversing a hypercube of volume $\Pi_{i=1}^{M} \delta Q_i$. Then, path independence means the entropy increment $\mathcal{S}_{\rm BOND}(\{Q_i\}|\{Q_i + \delta Q_i\})$ is independent of the order the edges are traversed in going from $\{Q_i\}$ to $\{Q_i + \delta Q_i\}$. Consider two possible paths labeled (1) and (2) along two of these coordinates $\{Q_i, Q_j\}$, as shown in Fig. 4. Along path (1), the entropy change to second order in $\delta Q$ is

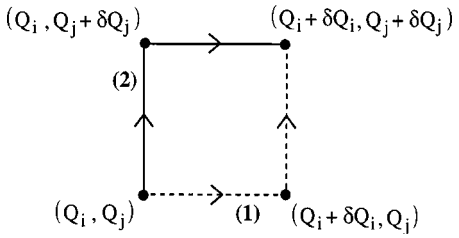


FIG. 4. Illustrating constraints on the functional form of the entropy, given it must be a state function. Path (1) dashed. Path (2) solid.

$$\mathcal{S}_{\rm BOND}^{(1)} = \int_{Q_i}^{Q_i + \delta Q_i} \delta Q_i' s_i(l_i, Q_i', Q_j) + \int_{Q_j}^{Q_j + \delta Q_j} \delta Q_j' s_j(l_j, Q_i + \delta Q_i, Q_j')$$

$$\cong s_i(l_i, Q_i, Q_j)\delta Q_i + s_j(l_j Q_i, Q_j)\delta Q_j + \frac{\delta Q_i^2}{2} \frac{\partial s_i}{\partial Q_i}(l_i, Q_i, Q_j) + \frac{\delta Q_j^2}{2} \frac{\partial s_j}{\partial Q_j}(l_j, Q_i, Q_j) + \delta Q_i \delta Q_j \frac{\partial s_j}{\partial Q_i}(l_j, Q_i, Q_j), \tag{3.13}$$

while along path (2) the entropy change is the same as expression (3.13) except that the last term is replaced by $\delta Q_i \delta Q_j (\partial s_i / \partial Q_j)(l_i, Q_i, Q_j)$. For these two expressions to be equal

$$\frac{\partial s_j}{\partial Q_i}(l_j, \{Q_k\}) = \frac{\partial s_i}{\partial Q_j}(l_i, \{Q_k\}) \quad \text{for} \quad i \neq j. \tag{3.14}$$

For $M$ dimensions, it follows that Eq. (3.14) holds for all pairs $(i,j)$, yielding $M(M-1)/2$ nontrivial constraints on the form of the configurational entropy loss at each value of $Q$.

When the entropy loss satisfies Eq. (3.14), the total entropy difference only depends on the initial and final states and can be rewritten as

$$\mathcal{S}_{\rm BOND}(\{Q_i^f\}|\{Q_i^o\}) = \sum_i \int_{Q_i^o}^{Q_i^f} dQ_i s_i(l_i, \{Q_j\}). \tag{3.15}$$

Now we seek an approximate formula for $s_i$ that satisfies Eq. (3.14). As mentioned above, we make a mean-field approximation to treat the entropics. Other treatments for the entropics are possible within the general framework, for example a spatially contiguous or capillarity nucleus,[25,26] or even an exact entropy functional taken from computational data.

In forming a contact $i$ from the unconstrained molten globule or coil state, the segment of polymer loses the entropy of a free chain with the length of that segment, $s_i(l_i, \{Q_j\} \cong \{0\}) = \ln(a/l_i)^{3/2}$, where $a$ is a $Q$-independent constant related through a sum rule to polymeric properties [see Eq. (3.24)]. However, contacts formed in a near-fully constrained polymer cost almost no entropy: $s_i(l_i, \{Q_j\} \approx \{1\}) \cong 0$. To account for this we introduce an effective loop length $l_{\rm EFF}(l_i, \{Q_j\})$ into $s_i(l_i, \{Q_j\}) = \ln(a/l_{\rm EFF})^{3/2}$. We ignore here possibly important changes in the power of the

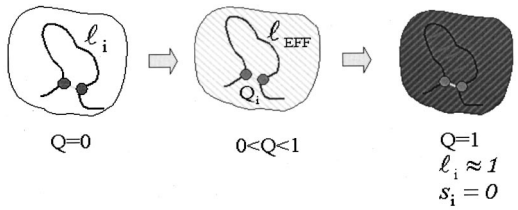


FIG. 5. Illustration of the mean-field approximation for calculating the entropy of loop closure in the presence of partial degrees of nativeness (see the text).

ideal chain exponent 3/2, since it becomes cumbersome to incorporate an exponent dependent on $\{Q_i\}$ and to simultaneously satisfy Eq. (3.14).

Because of the path independence of the configurational entropy loss $\mathcal{S}_{\mathrm{BOND}}(\{Q_i^f\}|\{Q_i^o\})$, the change in entropy for a small change in one of the contacts $Q_i^f \to Q_i^f + \delta Q_i$ is simply the integrand evaluated at the upper limit

$$\frac{\partial \mathcal{S}_{\mathrm{BOND}}}{\partial Q_i}(\{Q_j^f\}|\{Q_j^o\}) = s_i(l_i, \{Q_k^f\}), \tag{3.16}$$

which can be shown from Eqs. (3.14) and (3.15) by using the definition of the derivative.

In this paper we satisfy Eq. (3.14) with the following ansatz for the functional form of $l_{\mathrm{EFF}}$:

$$l_{\mathrm{EFF}}(l_i, \{Q_k\}) = f(l_i) g(\{Q_k\}) = f(l_i) g\left(\frac{1}{M}\sum_k Q_k\right), \tag{3.17}$$

so that the loop length is decreased by a function of the mean of the contact density field, $g(Q)$. This is in the spirit of the Hartree ansatz in the one-electron theory of metals, where electrons interact only through an averaged field (see Fig. 5). The condition $l_{\mathrm{EFF}}(l_i, Q=0) = l_i$ gives $f(l_i) = l_i$ and $g(0) = 1$. The condition that $l_{\mathrm{EFF}}(l_i, Q=1) \approx 1$ gives $g(1) \approx 1/\bar{l}$ [since $g(Q)$ cannot depend on $l_i$], where $\bar{l} = (1/M)\Sigma_i l_i$. To approximate the $Q$ dependence of $l_{\mathrm{EFF}}$, let the probability that a monomer is constrained at $Q$ be $\mathcal{Q}$, under the assumption of a uniform contact probability. Then, given a chain of unbonded monomers, the probability of it being length $L$ is then $p_L = \mathcal{Q}(1-\mathcal{Q})^{L-1}$. So, the average length of strings of unbonded monomers at $Q$ is then $\bar{L} = \Sigma_L L p_L / \Sigma_L p_L \cong 1/\mathcal{Q}$. For low values of $Q$, $\mathcal{Q} \cong 2M/N = 2zQ$, while for high values $Q$, $\mathcal{Q} \cong Q$.[87] We do not go into detail on this issue here; instead, we approximate $\mathcal{Q} \cong Q$ for all values of $Q$. Then, $\bar{L} = 1/Q$ can be interpreted roughly as the total length of polymer $N$ over the total number of constrained monomers at $Q$. We approximate the effective loop length at $Q$, $l_{\mathrm{EFF}}(l_i, Q)$, in the same way by dividing the total loop length $l_i$ by the number of constrained residues in the loop $\cong \bar{l}Q$, so that finally

$$s_i(l_i, \{Q_k\}) \approx \frac{3}{2}\ln\left(\frac{a}{l_{\mathrm{EFF}}(l_i, Q)}\right), \tag{3.18}$$

$$l_{\mathrm{EFF}}(l_i, Q) \approx \frac{l_i}{(\bar{l}-1)Q + 1}. \tag{3.19}$$

The quantity $l_{\mathrm{EFF}}$ is the renormalized loop length after tracing over all configurations with a fixed fraction $Q$ of native contacts. The number of non-native contacts is not fixed, and their presence does not reduce the *configurational* entropy, so they need not be considered here. Their effect on the thermal entropy is accounted for in Eq. (3.8). Note that $l_{\mathrm{EFF}}$ has the mean-field behavior when $l_i \to \bar{l}$ and $\bar{l}$ is large, and also has the right limiting behavior as $Q \to 0$ and approximate limiting behavior when $Q \to 1$. Equations (3.19) and (3.18) are accurate for weak dispersion in loop lengths; for larger values of $\delta l_i$ they must be modified [see the comments after Eq. (3.28)].

Expressions (3.15) and (3.18) reduce to the Flory form for the configurational entropy loss in the mean-field limit when $l_i = \bar{l}$ and $Q_i = Q$. Then, Eq. (3.15) becomes

$$\mathcal{S}_{\mathrm{BOND}}^{(\mathrm{MF})}(Q|0) = \int_0^Q dQ\, M \ln\left(\frac{a[1+(\bar{l}-1)Q]}{\bar{l}}\right)^{3/2}, \tag{3.20}$$

which can be interpreted as a summation of entropy losses from 0 to $Q$

$$\begin{aligned}\mathcal{S}_{\mathrm{BOND}}^{(\mathrm{MF})}(Q|0) &= \sum_{Q'=\Delta Q}^{Q} \Delta S(Q') \\ &= \sum_{Q'=\Delta Q}^{Q} \ln\frac{\Omega(Q')}{\Omega(Q'-\Delta Q)} \\ &= \ln\left(\frac{\Omega(\Delta Q)}{\Omega(0)}\frac{\Omega(2\Delta Q)}{\Omega(\Delta Q)}\cdots\frac{\Omega(Q)}{\Omega(Q-\Delta Q)}\right) \\ &= \ln\frac{\Omega(Q)}{\Omega(0)} = S^{(\mathrm{MF})}(Q) - S^{(\mathrm{MF})}(0).\end{aligned}$$

When $\bar{l}Q \gg 1$, Eq. (3.20) gives

$$\frac{\mathcal{S}_{\mathrm{BOND}}^{(\mathrm{MF})}}{M}(Q|0) = \frac{3Q}{2}(\ln a - 1 + \ln Q), \tag{3.21}$$

which is essentially the Flory result derived earlier in the mean-field limit.[87,91,92]

In the presence of heterogeneity, Eqs. (3.15) and (3.18) give

$$\begin{aligned}\mathcal{S}_{\mathrm{BOND}}(\{Q_i\}|0) &= \frac{3}{2}MQ\ln a - \sum_{i=1}^{M} Q_i \ln l_i \\ &\quad + \sum_{i=1}^{M}\int_0^{Q_i} dQ_i' \ln\left[1 + \frac{\bar{l}-1}{M}\sum_k Q_k\right] \\ &= \frac{3}{2}M\left(Q(\ln a) - \frac{1}{M}\sum_i Q_i \ln l_i - Q\right. \\ &\quad \left. + \frac{[1+(\bar{l}-1)Q]}{\bar{l}-1}\ln[1+(\bar{l}-1)Q]\right),\end{aligned} \tag{3.22}$$

where the last integral can be done by charging up each $Q_i$ one at a time (in any order) to its value at $Q$, i.e., the integral is $\Sigma_i \int_0^{Q_i} dQ_i' \ln[1+(\overline{l}-1/M)(\Sigma_{j<i}Q_j+Q_i')]$. This gives an expression identical to the mean-field result for this term, since the integrand only depends on $Q$ and is integrated up to each $Q_i(Q)$.

Because the free energy of the native state $F(\{1\}|\{\epsilon_i\},\{l_i\})$ is $E_N$ [cf. Eq. (3.8)], all the polymer entropy is lost upon folding in the model. Therefore, there is a sum rule for the entropy loss

$$\mathcal{S}_{\mathrm{BOND}}(\{1\}|0)=\sum_{i=1}^{M}\int_0^1 dQ_i\, s_i(l_i,\{Q_j\})=-N\ln\nu=-Ns_o, \tag{3.23}$$

which, using Eq. (3.22), determines the coefficient $a$ in the entropy of bond formation

$$\ln a(\nu,\{l_i\})=-\frac{2}{3}\frac{s_o}{z}+1+\overline{\ln l}-\frac{\overline{l}}{\overline{l}-1}\ln\overline{l}. \tag{3.24}$$

The coefficient $a$ depends on the distribution of $l_i$ as well as the entropy per monomer $s_o$. Using (3.24) and (3.22), the final expression for the entropy loss arising from contact formation is

$$\mathcal{S}_{\mathrm{BOND}}(\{Q_i\}|0)=\mathcal{S}_{\mathrm{MF}}(Q,\overline{l})-\tfrac{3}{2}M\langle\delta Q\,\delta\ln l\rangle, \tag{3.25}$$

where the first term in (3.25) is the mean-field entropy loss

$$\mathcal{S}_{\mathrm{MF}}(Q,\overline{l})=-QNs_o-\frac{3}{2}MQ\frac{\overline{l}\ln\overline{l}}{\overline{l}-1}+\frac{3}{2}M\frac{1}{\overline{l}-1}\times[1+(\overline{l}-1)Q]\ln[1+(\overline{l}-1)Q], \tag{3.26}$$

and the second term in (3.25) is the change in entropy loss due to fluctuations (again the notation $\langle X_i\rangle\equiv\overline{X}\equiv 1/M\Sigma_i X_i$ is used)

$$M\langle\delta Q\,\delta\ln l\rangle=\sum_i (Q_i-Q)(\ln l_i-\overline{\ln l}). \tag{3.27}$$

From inspection of Eqs. (3.25)–(3.27), we can confirm that $\mathcal{S}_{\mathrm{BOND}}(Q=0)=0$ and $\mathcal{S}_{\mathrm{BOND}}(Q=1)=-Ns_o$. When $\overline{l}Q\gg 1$, (3.26) reduces to Eqs. (3.21) and (3.24)

$$\mathcal{S}_{\mathrm{MF}}(Q,\overline{l}\gg 1)\approx -QNs_o+\tfrac{3}{2}zNQ\ln Q, \tag{3.28}$$

which has lost the information about the mean loop length and only retained information about the total chain length $N$, as in the Flory mean-field theory. The first term in (3.26) or (3.28) is the loss in entropy to constrain a given fraction of the protein and is linear in $Q$. The remainder in (3.26) or (3.28) is the extra entropy loss this constraint induces on the remaining free parts by pinning down regions of the polymer chain. The analogous quantity in the capillarity theory is the surface entropy cost in forming a nucleus of folded structure.[25,93] In capillarity theories, the surface entropy cost scales like $N^{2/3}$, whereas in mean-field theories it scales like $N$. Equation (3.26) can be thought of as a generalization of Eq. (3.28) to finite mean return length $\overline{l}$ for a finite-sized system, and Eq. (3.25) can be thought of as generalizing (3.26) to include variations in the return length.

The effect of these fluctuations or variations in (3.25) is typically to increase the bond entropy of partially native states. Forming entropically likely contacts with higher probability leaves more residual entropy than if all contacts are taken to have the same return length and formation probability, as in the mean-field approximation. The trend in the folding barrier with heterogeneity results from the interplay of this effect with the effects of fluctuations on the route entropy and native energetic fluctuations. The magnitude of the effect scales extensively with the size of the system. To illustrate, recall that for a Gō model the total entropy at $Q$ is $Ns_o+\mathcal{S}_{\mathrm{ROUTE}}(\{Q_i\})+\mathcal{S}_{\mathrm{BOND}}(\{Q_i(Q)|0\})$ [cf. Eqs. (3.6) and (3.7)]. Thus, if we look at loops longer than the average ($l_i>\overline{l}$, and since the log function is concave down, $\ln l_i>\overline{\ln l}$), then they are less likely to be formed [cf. Eq. (3.34)], so that $Q_i<Q$ and the second term in (3.25) is negative, thus raising the bond entropy. If $l_i<\overline{l}$, $Q_i>Q$ and the effect is the same. The halo entropy of the system $Ns_o+\mathcal{S}_{\mathrm{BOND}}(\{Q_i(Q)|0\})$ increases when we relax the condition that all contacts must be equally probable, and allow differences in contact probability based on their entropic likelihood.

From (3.28) it can be seen that there is an entropy crisis ($\mathcal{S}_{\mathrm{MF}}<0$) at values of $Q<1$ when $2s_o/3z\lesssim 1$. However, the entropy in Eq. (3.25) is interpreted as being decomposed into two terms, only the sum of which is physically meaningful. The first term is an idealization, and the second term describes deviations from that ideal model when realistic fluctuations are accounted for. Here, these fluctuations alleviate the problem of the entropy crisis. A regime where one term in the expression for the entropy is negative is an indication that it may be more meaningful to develop an expression starting from a different limit, e.g., perturbing from the fully constrained (native) conformation.[24] Typical values of the parameters from off-lattice simulations of chymotrypsin inhibitor or the $\alpha$-spectrin SH3 domain[45] give $s_o\cong 3.4$, $z\cong 2.4$, $2s_o/3z\cong 0.94$; here, the entropy crisis occurs rather late in folding, if at all, because of entropy increase by the above-mentioned effects.

On the other hand, Eq. (3.18) breaks down for sufficiently large structural heterogeneity. Inspection of (3.18) shows that the entropy loss has the same derivative as a function of $Q$ for all contacts, but the initial values are different. This leads to some problems with the shorter loops for high $Q$ values, which is worth noting as a word of caution here. The crude way in which the entropy loss for a loop is coupled to the degree of nativeness of the rest of the protein leads to a non-negative entropy change to close some of the shorter loops near $Q\approx 1$. We resolved this problem by actually truncating the entropy loss formula for the shorter loops when they reached a value of zero. Putting Eq. (3.24) into (3.18), letting $\overline{l}Q\gg 1$, and expanding to first order in $\delta l/\overline{l}$ (weak dispersion limit), we obtain the approximate value of $Q$ where the entropy loss crosses zero, namely $Q_{\mathrm{S}}\approx 2s_o/3z+\delta l_i/\overline{l}$. When $\delta l_i=0$ this is consistent with the Flory analysis above; however, when $\delta l_i<0$ (shorter loops) $Q_{\mathrm{S}}$ is de-

creased. We truncate the entropy formula at zero for $Q > Q_S$.

As a simple illustration of how dispersion in loop lengths affects $Q_S$, consider a structure whose loop distribution is given by first returns of a random walk, $P(l) \approx (3/2)l^{-5/2}$, and thus from Eq. (3.18) $P(s) = \exp(s - s(l_i = 1))$, where $s(l_i = 1) = 5/2 - (9/4)\ln 3 - s_o/z + (3/2)\ln(1+2Q)$ is the entropy of closure for the smallest loops (where the problem is the worst). Using the above values for $s_o$ and $z$, all $s_i$ are negative until $Q_S \gtrsim 0.76$. Since the barrier peak typically occurs at $Q$ values smaller than this, errors due to truncation would be small for these structures. Deviations from the random walk distribution arising from regularities in return length for real protein structures also alleviate the problem slightly.[94] On the other hand, protein structures tend to have distributions with a wider dispersion than the random globule, and in these cases the problem would be worse. Applying the theory to the lattice structure of Fig. 1, we must truncate the entropy loss for loops with $l_i = 3$ at $Q_{S3} \approx 0.4$ and for loops with $l_i = 5$ at $Q_{S5} \approx 0.75$; for all other loops there is no entropy crisis. Numerically there is some quantitative error introduced by this truncation, since in the theory these loops no longer contribute to the total entropy loss above $Q_S$, whereas in the actual simulation they do. Of course, implementing a cutoff in loop entropy causes the total entropy to deviate from a state function by Eq. (3.14). Theories of polymer entropy which take more complete account of correlations should remedy this and are a topic of future work. For now we content ourselves with the Hartree-style entropy formulation in Eq. (3.18), implementing a cutoff if needed. In general, however, the barrier height still shows the same decreasing trend with heterogeneity whether this approximate entropy formulation is used, or whether the computational entropy taken from the lattice model is used.[49,52]

### C. The free-energy functional

Equations (3.8), (3.11a), and (3.25) together give an analytic expression for the free energy for a fast-folding protein which includes heterogeneity in the folding mechanism

$$F(\{Q_i(Q)\}|\{\epsilon_i\},\{l_i\}) = F_{MF}(Q,\overline{\epsilon},\overline{l}) + \delta F(\{\delta Q_i\}|\{\delta\epsilon_i\},\{\delta l_i\}), \tag{3.29}$$

where we have written the total free energy in terms of a mean-field term plus a fluctuation due to variations in energy, loop length, and contact probability. In (3.29), $F_{MF}/M$ is the mean-field free energy per monomer[24]

$$\frac{F_{MF}}{M} = \overline{\epsilon}Q - T\frac{s_o}{z} - t\frac{\mathcal{S}_{MF}}{M}(Q,\overline{l}) - T\frac{\mathcal{S}_{ROUTE}}{M}(Q) - \frac{b^2}{2T}(1-Q) + \frac{\overline{E}}{M}, \tag{3.30}$$

with $\mathcal{S}_{MF}$ given by Eq. (3.26), and $\mathcal{S}_{ROUTE}$ given by Eq. (3.11a) with all $Q_i = Q$. The fluctuation in (3.29) is given by

$$\frac{\delta F}{M}(\{\delta Q_i\}|\{\delta\epsilon_i\},\{\delta l_i\}) = \langle \delta Q\, \delta\epsilon\rangle + T\lambda(Q)\left\langle Q_i \ln\frac{Q_i}{Q} + (1-Q_i)\ln\frac{1-Q_i}{1-Q}\right\rangle + \tfrac{3}{2}T\langle \delta Q\, \delta \ln l\rangle. \tag{3.31}$$

The mean-field free energy in Eq. (3.30) contains six parameters which characterize the system: $N$, $s_o$, $z$, $b$, $\overline{E}$, and $\alpha$ [which appears in $\lambda(Q)$ of Eq. (3.11b)]. Once chosen, these parameters are fixed for the rest of the analysis. Equation (3.31) has no new adjustable parameters. All other quantities such as $\overline{\epsilon}$, $\overline{l}$, $\delta l^2$, etc. arise from the structural and energetic distribution of a given protein at overall nativeness $Q$ and temperature $T$. In the analysis here, we study trends in the thermodynamics by varying these distributions.

The free-energy functional consists of an integration over a free-energy density whose only information about the surrounding medium is through the average field present ($Q$): $F = \Sigma_i f_i(Q_i, Q)$. Explicitly accounting for cooperative entropic effects due to correlations between contacts[39,51,95,96] would be an important extension of the model, and terms that lead to such effects have been introduced into the functional in similar models.[39,51]

We can now investigate the effects of heterogeneity on each of the three terms in Eq. (3.31). As mentioned above, for longer loops the contact probability is expected to be less than average, and for shorter loops $Q_i$ is expected to be above average. So, relaxing the $Q_i$ values to accommodate this makes the third term on the right-hand side of (3.31) negative, lowering the free energy. Also, since the fluctuation $\delta Q_i$ is expected to be positive when a contact is stronger ($\delta\epsilon_i$ is negative), the first term on the right-hand side of (3.31) is negative and the free energy is lowered. Last, the second term in Eq. (3.31) consists of two terms inside the average which are both concave up, i.e., have a positive second derivative with respect to $Q_i$. Thus, the average of the terms is greater than the term evaluated at the average, i.e.,

$$\left\langle Q_i \ln\frac{Q_i}{Q}\right\rangle > \langle Q_i\rangle \ln\frac{\langle Q_i\rangle}{Q} = 0, \qquad \left\langle (1-Q_i)\ln\frac{1-Q_i}{1-Q}\right\rangle > (1-\langle Q_i\rangle)\ln\frac{1-\langle Q_i\rangle}{1-Q} = 0, \tag{3.32}$$

and so the second term in (3.31) is positive. Fluctuations away from uniform ordering raise the terms in the free energy due to route entropy.[97] This effect competes with the two lowering effects above. To find which terms dominate, we find the functional dependence of the contact probabilities $Q_i$ on the energies $\epsilon_i$ and entropies $s_i$ in the next subsection, and then investigate the trend on barrier height under variations of $\epsilon_i$ and $s_i$ in Sec. IV.

### D. The most likely distribution of contact probabilities

Equations (3.29), (3.30), and (3.31) describe the free energy for an arbitrary distribution of contact probabilities $\{Q_i(Q)\}$, subject only to the constraint that the average probability $\langle Q_i\rangle$ is $Q$. The most likely distribution $\{Q_i^*(Q)\}$ of the contact probabilities $Q_i(Q)$, i.e., the thermal distribution, is obtained by minimizing the free energy $F(\{Q_i(Q|\{\epsilon_i\},\{l_i\})\})$ subject to the constraint $\Sigma_i Q_i(Q) = MQ$, i.e., $\delta(F+\mu\Sigma_j Q_j)=0$, or

$$\sum_i \left[\frac{\partial}{\partial Q_i}F(\{Q_i\}|\{\epsilon_i\},\{l_i\})+\mu\right]\delta Q_i=0, \tag{3.33}$$

for arbitrary and independent variations $\delta Q_i$. Substituting Eqs. (3.29), (3.30), and (3.31) into Eq. (3.33) yields a Fermi–Dirac distribution for the most probable thermodynamic occupation probabilities $\{Q_i^*\}$ for a given $\{\epsilon_i\}$ and $\{l_i\}$

$$Q_i^*(Q,\{\epsilon_i\},\{l_i\})=\frac{1}{1+\exp\left[\frac{1}{\lambda T}\left(\mu+\epsilon_i-Ts_i(l_i,Q)-T\lambda'\langle s^o_{\mathrm{ROUTE}}\rangle+\frac{b^2}{2T}\right)\right]}, \tag{3.34}$$

where $\lambda'=d\lambda(Q)/dQ$ [cf. Eq. 3.11b] and $\langle s^o_{\mathrm{ROUTE}}\rangle(Q) = \langle -Q_j\ln Q_j-(1-Q_j)\ln(1-Q_j)\rangle$. Thus, each probability $Q_i^*$, referred to below simply as $Q_i$, is a function of all the $\{Q_j\}$, and must be solved for self-consistently. Non-native ruggedness introduces a term with anomalous $1/T^2$ temperature dependence in the distribution. By the structure of Eq. (3.34), all contact probabilities $Q_i$ are between zero and 1.

The Lagrange multiplier $\mu$ is determined by the constraint $\Sigma_i Q_i^*=MQ$, and so is a function of $Q$ and the distributions of $\{\epsilon_i\}$ and $\{l_i\}$. It can be interpreted as proportional to an effective force along the $Q$ coordinate, since

$$\mu=-\frac{1}{M}\frac{\partial F}{\partial Q} \tag{3.35}$$

by the properties of the Legendre transformation (see the Appendix). Thus again, since the free energy $F$ is of course a function of $Q$ and the distributions $\{\epsilon_i\}$ and $\{l_i\}$, $\mu = -(1/M)\partial F/\partial Q$ also.

The second variation of $F(\{Q_i\}|\{\epsilon_i\},\{l_i\})$ [neglecting terms of order $\mathcal{O}(1/M)$] is indeed positive

$$\frac{\partial^2 F}{\partial Q_j\partial Q_i}=\lambda T\frac{\delta_{ij}}{Q_i(1-Q_i)}>0, \tag{3.36}$$

verifying that the extremal values of $Q_i$ are the ones which minimize $F(\{Q_i\}|\{\epsilon_i\},\{l_i\})$.

## IV. CHANGING FOLDING MECHANISMS BY TAILORING NATIVE INTERACTION ENERGIES AND ALTERING NATIVE STRUCTURAL MOTIFS

Most single domain proteins must fold over a free-energy barrier of a few $k_BT$ at the transition temperature. This barrier is small compared to the total thermal energy in the system, reflecting the exchange of energy for entropy as a protein folds.[24,98] However, the barrier height can vary significantly depending on which parts of a protein are most stable in the native structure, i.e., how the native energy is distributed throughout the native structure. In Sec. IV A we look at the effects on the thermodynamics when native interactions are changed in a controlled manner. We find that a distribution of native energy which induces a uniform folding mechanism will maximize the barrier. Increasing heterogeneity in the folding mechanism systematically decreases the folding barrier and may eliminate it entirely, at least in the absence of cooperative interactions. The corresponding folding rate increases, as long as the protein remains well designed. In Sec. IV B we develop a perturbation expansion of the free energy to incorporate structural as well as energetic heterogeneity, and the effect on the free energy of correlations between them. In Sec. IV C we illustrate the effect of contact order or mean contact length on the folding barrier in the model, and in Sec. IV D we investigate the effects of structural variance on a hypothetical ensemble of well-designed protein fold motifs. We find that for fixed average loop length $\overline{l}$, native structures that have larger dispersion $\delta l$ in the distribution of return lengths tend to have smaller folding barriers. In Sec. IV E we show how the folding barrier decreases with the degree of route-like folding in the system, so long as the protein remains well designed.

### A. Energetic heterogeneity for a given structure

First, we consider the free energy as a function of $Q$ and the field of energies $\{\epsilon_i\}$, given the field of loop lengths $\{l_i\}$. Each contact probability $Q_i$ in the Free-energy Eq. (3.29) is considered through Eq. (3.34) to be a function of $Q$, its energy, its loop length, and the Lagrange multiplier $\mu(Q,\{\epsilon_j\},\{l_j\})$, which is itself a function of $Q$ and the distributions $\{\epsilon_j\}$ and $\{l_j\}$. Thus, the free energy depends both implicitly and explicitly on $\{\epsilon_i\}$.

We now seek to tune the values of $\{\epsilon_i\}$, at fixed stability (fixed total native energy)

$$\sum_j \epsilon_j=E_N, \tag{4.1}$$

$$\sum_j \delta\epsilon_j=0, \tag{4.2}$$

to the distribution $\{\epsilon_i^*(\{l_j\})\}$ that extremizes the free-energy barrier. Under variations of the energies $\{\delta\epsilon_i\}$ for a given structure $\{l_i\}$, the free energy becomes

$$F\{\epsilon_{io}+\delta\epsilon_i\}=F\{\epsilon_{io}\}+\sum_i\left(\frac{\delta F}{\delta\epsilon_i}\right)_{\epsilon_{io}}\delta\epsilon_i + \frac{1}{2!}\sum_{i,j}\left(\frac{\delta^2 F}{\delta\epsilon_i\delta\epsilon_j}\right)_{\epsilon_{io},\epsilon_{jo}}\delta\epsilon_i\delta\epsilon_j+\cdots, \tag{4.3}$$

where $\delta/\delta\epsilon_i$ is the total derivative with respect to $\epsilon_i$. So, the distribution $\{\epsilon_i^*(\{l_j\})\}$ that extremizes the free-energy barrier subject to the constraint Eq. (4.1) is the solution of $\delta(\Delta F^{\ddagger}-p\Sigma_j\epsilon_j)=0$, or

$$\sum_i\left[\frac{\delta\Delta F^{\ddagger}}{\delta\epsilon_i}-p\right]\delta\epsilon_i=0, \tag{4.4}$$

for arbitrary and independent variations $\delta\epsilon_i$ in the energies. The Lagrange multiplier $p$ imposes the constraint that the total native energy $E_{\mathrm{N}}$ is constant. Changes in the barrier height are roughly equal to changes in the free energy at the barrier peak, since the free energy in the unfolded state $Q_o\approx 0$ is more weakly dependent on $\{\epsilon_i\}$, i.e., $\delta\Delta F^{\ddagger}/\delta\epsilon_i\cong\delta F(Q^{\ddagger})/\delta\epsilon_i$, because $\delta F(Q_o\approx 0)/\delta\epsilon_i\cong 0$; less native structure is present in the unfolded state. The effect on the free energy due to perturbations in $\{\epsilon_i\}$ is largest at intermediate $Q$; there is no effect at the end points because at $Q=0$ there are no native interactions, and at $Q=1$ all native interactions are present and must add up to the total native stability $E_{\mathrm{N}}$, which is fixed. In fact in the equations for the free-energy perturbation this effect is manifested by the factor of $Q(1-Q)$ which multiplies every term, see, e.g., Eqs. (4.19) and (4.34).

Because of the implicit functions mentioned above

$$\frac{\delta F}{\delta\epsilon_i}=\frac{\partial F}{\partial\epsilon_i}+\sum_j\frac{\partial F}{\partial Q_j}\frac{\partial Q_j}{\partial\epsilon_i}+\sum_j\frac{\partial F}{\partial Q_j}\frac{\partial Q_j}{\partial\mu}\frac{\partial\mu}{\partial\epsilon_i} \tag{4.5}$$

$$=\frac{\partial F}{\partial\epsilon_i}+\mu\sum_j\left[\frac{\partial Q_j}{\partial\epsilon_i}+\frac{\partial Q_j}{\partial\mu}\frac{\partial\mu}{\partial\epsilon_i}\right]. \tag{4.6}$$

However, the term in square brackets is just the total derivative $\delta Q_j/\delta\epsilon_i$, so the sum vanishes because $Q$ is a fixed parameter independent of $\epsilon_i$[99]

$$\sum_j\frac{\delta Q_j}{\delta\epsilon_i}=\frac{\delta}{\delta\epsilon_i}\sum_j Q_j=\frac{\delta}{\delta\epsilon_i}(MQ)=0. \tag{4.7}$$

Differentiating Eq. (3.8) immediately yields

$$\frac{\partial\Delta F^{\ddagger}}{\partial\epsilon_i}\cong Q_i(Q^{\ddagger}), \tag{4.8}$$

so the perturbative change in the free-energy barrier by varying a contact's energy is equal to the probability that contact was formed at $Q^{\ddagger}$.

This is closely related to experimental $\phi_i$ values, which measure the change in the log folding rate $k_{\mathrm{F}}$ [cf. Eq. (1.1)] after mutation over the change in difference in equilibrium populations of the folded and unfolded states[59,100]

$$\phi\equiv\frac{\delta\ln(k_{\mathrm{F}}/k_o)}{\delta\Delta F_{\mathrm{F}}}. \tag{4.9}$$

Experimental measurements of quantities more closely related to $Q_i$ may be made by performing double mutations.[63,100] This method measures changes in rate and stability after mutating two residues in proximity, then subtracts the sum of the changes after mutating each residue separately, thus effectively measuring the rate/stability change due specifically to the interaction between the residues (rate/stability changes due to varying $\epsilon_i$ in our language). When the prefactor to the rate is unaffected by the mutation, this is equivalent to the change with mutation in the barrier height over the change in the difference of the free-energy minima,[20,59] which we refer to as $\phi'$

$$\phi_i'\equiv\frac{(\partial F^{\neq}/\partial\epsilon_i)-(\partial F_u/\partial\epsilon_i)}{(\partial F_f/\partial\epsilon_i)-(\partial F_u/\partial\epsilon_i)}=\frac{Q_i(Q^{\ddagger})-Q_i(Q_U)}{Q_i(Q_F)-Q_i(Q_U)}. \tag{4.10}$$

When the nativeness in the unfolded state can be neglected, $Q_i(Q_U)\approx 0$, and when the native contacts in the folded state are essentially fully formed, $Q_i(Q_F)\approx 1$. Then, Eq. (4.10) becomes

$$\phi_i'\equiv\frac{\delta\Delta F^{\neq}}{\delta\epsilon_i}=\frac{\partial\Delta F^{\neq}}{\partial\epsilon_i}=Q_i(Q^{\ddagger}). \tag{4.11}$$

Comparing $\phi$ values with contact probabilities assumes the use of contact probability as a kinetic reaction coordinate. In fact, it has been observed for lattice simulations that $\phi$ values correlate with $Q_i$ values as well as any other reaction coordinate currently proposed.[101]

Continuing now to find the energies $\epsilon_i^*$ which extremize the free energy, Eq. (4.4) gives finally: $Q_i(Q^{\ddagger},\ \mu^{\ddagger}=0,\epsilon_i^*,l_i)=p$: the free energy is extremized when all the $Q_i$ values are tuned to the same number at the barrier peak. This folding scenario is that of a symmetric funnel: the protein is equally likely to order from any place within it. Thus, since $\Sigma_i Q_i=MQ$

$$Q_i(Q^{\ddagger},\mu^{\ddagger}=0,\epsilon_i^*,l_i)=Q^{\ddagger}. \tag{4.12}$$

Solving Eq. (4.12) for the energies using Eq. (3.34) gives

$$\epsilon_i^*=Ts_i+T\frac{d}{dQ}(\lambda[-Q\ln Q-(1-Q)\ln(1-Q)])_{Q^{\ddagger}}-\frac{b^2}{2T}. \tag{4.13}$$

Subtracting $\overline{\epsilon}$ from $\epsilon_i$ by averaging Eq. (4.13) yields

$$\epsilon_i^*-\overline{\epsilon}=T(s_i-\overline{s}) \tag{4.14a}$$

$$=-\tfrac{3}{2}T(\ln l_i-\overline{\ln l}), \tag{4.14b}$$

where Eq. (3.19) was used to obtain Eq. (4.14b). The free-energy fluctuations $\delta f_i=0$ in a uniform folding mechanism. Thus, contacts pinching off longer loops ($l_i\gtrsim\overline{l_i}$) have lower (stronger) energies ($\epsilon_i<\overline{\epsilon_i}$) to make all the contact probabilities equal at the barrier peak.[102] If correlations between contacts are fully accounted for, the $Q_i$ values deviate slightly

from $Q$ away from the barrier peak, but the fluctuations away from uniform ordering are still strongly suppressed.[49]

Evaluating the second derivative stability matrix in Eq. (4.3) shows $Q_i = Q^\ddagger$ in Eq. (4.12) to be an unstable maximum, as follows. From Eq. (4.8)

$$\frac{\delta^2 F}{\delta\epsilon_j \delta\epsilon_i} = \frac{\delta Q_i}{\delta\epsilon_j} = \frac{\partial Q_i}{\partial\epsilon_j} + \frac{\partial Q_i}{\partial\mu}\frac{\partial\mu}{\partial\epsilon_j} = -\frac{Q_i(1-Q_i)}{\lambda T}\left(\delta_{ij} + \frac{\partial\mu}{\partial\epsilon_j}\right), \tag{4.15}$$

by Eq. (3.34). Thus, the second-order change in the free energy at the extremum is

$$\sum_{i,j}\left(\frac{\delta^2\Delta F^\ddagger}{\delta\epsilon_j\delta\epsilon_i}\right)_{\epsilon_i^*,\epsilon_j^*}\delta\epsilon_i\delta\epsilon_j = -\frac{Q^\dagger(1-Q^\dagger)}{\lambda T}\left[M\overline{\delta\epsilon^2} + \sum_{i,j}\left(\frac{\partial\mu}{\partial\epsilon_j}\right)\delta\epsilon_i\delta\epsilon_j\right]. \tag{4.16}$$

Since the perturbations $\delta\epsilon_i$ are independent, cross terms in the double sum of Eq. (4.16) vanish, making the sum equal to

$$\sum_{i=1}^{M}\left(\frac{\partial\mu}{\partial\epsilon_i}\right)\delta\epsilon_i^2. \tag{4.17}$$

This term is negligible for the following reasons. First, note that $\partial F/\partial\epsilon_i = Q_i$ is $\sim\mathcal{O}(1)$. Then, since $\partial\mu/\partial\epsilon_i = -(1/M)\times(\partial/\partial Q)(\partial F/\partial\epsilon_i)$ by Eq. (3.35), the terms $\partial\mu/\partial\epsilon_i$ in Eq. (4.17) are $\sim\mathcal{O}(1/M)$. So, the sum of $M$ terms in (4.17) is $\sim\mathcal{O}(1)\overline{\delta\epsilon^2}$, whereas the first term in Eq. (4.16) is $\sim\mathcal{O}(M)\overline{\delta\epsilon^2}$ and dominates in the thermodynamic limit. Thus, to order $\mathcal{O}(1/M)$

$$\left(\frac{\delta^2\Delta F^\ddagger}{\delta\epsilon_j\delta\epsilon_i}\right)_{\epsilon_i^*,\epsilon_j^*} = \left(\frac{\partial Q_i}{\partial\epsilon_j}\right)_{\epsilon_i^*,\epsilon_j^*} = -\delta_{ij}\frac{Q^\ddagger(1-Q^\ddagger)}{\lambda^\ddagger T}, \tag{4.18}$$

which is clearly negative, meaning that tuning the energies so that $Q_i = Q^\ddagger$ maximizes the free energy at the barrier peak. The extremizations have been done for an arbitrary $Q$, and we need not additionally extremize to find the barrier position. Wherever the barrier is, whether or not it is moving around as the $\epsilon_i$ change, its free energy is going down. To actually calculate the change in barrier height nonperturbatively, we can calculate the free energy for all $Q$ and then extremize to find the unfolded minimum and the maximum at the barrier peak. This is what is done in Fig. 9.

Substituting Eqs. (4.8), (4.12), and (4.18) into (4.3) gives the perturbative expression for the change in barrier height

$$\Delta F^\ddagger\{\epsilon_i^* + \delta\epsilon_i\} \cong \Delta F_{\mathrm{MF}}^\ddagger - M\frac{Q^\ddagger(1-Q^\ddagger)}{2\lambda^\ddagger T}\overline{\delta\epsilon^2}. \tag{4.19}$$

For an energetic standard deviation of about a $k_BT$ from the optimal distribution, the barrier goes down by about $\sim Nk_BT/2$ [we've let $M\approx 2N$, $\lambda^\ddagger\approx 1-Q^\ddagger$ since the exponent $\alpha$ in (3.11b) is about 1, and $Q^\ddagger\approx 1/2$]. The barrier governed rate increases with energetic variance from the optimal distribution as

$$k = k_o\exp\left(-\frac{\Delta F^\ddagger}{T}\right) = k_{\mathrm{HOMO}}\exp\left(Q^\ddagger(1-Q^\ddagger)\frac{M\overline{\delta\epsilon^2}}{2\lambda^\ddagger T^2}\right). \tag{4.20}$$

A similar result may be obtained through the following intuitive argument. Consider making random energetic perturbations on the contact energies of an initially homogeneous idealized system (where all contact probabilities are the same: $Q_i = Q$) with free-energy barrier $F_{\mathrm{HOMO}}$ and folding rate $k_o\exp(-F_{\mathrm{HOMO}}/T)$. Then, the new rate is

$$k_f = k_o\exp\left(-\frac{F_{\mathrm{HOMO}} + \delta F(T)}{T}\right) = k_{\mathrm{HOMO}}\exp\left(-\frac{\delta F(T)}{T}\right), \tag{4.21}$$

where again we have ignored the change in prefactor as being a smaller effect. If the total native (unconstrained) energetic variance $\Sigma_i\delta\epsilon_i^2$ is $\Delta E_{\mathrm{N}}^2$, the variance in native core energies at the transition state is approximately $\Delta E_{\mathrm{N}}^{2\neq} = Q^\ddagger(1-Q^\ddagger)\Delta E_{\mathrm{N}}^2$, given that the energies must sum to total native energy $E_{\mathrm{N}}$. The variance vanishes at $Q=0$ since there are no native contacts made there, and vanishes at $Q=1$ since all the $\Sigma_i\epsilon_i = E_{\mathrm{N}}$, i.e., all the energies must sum to a fixed number and thus their sum cannot vary. Approximating the transition state as an ensemble of states with uncorrelated energies, i.e., a random energy model,[103] and considering only the effects of changing native interactions, the energy will always decrease twice as much as the entropy times the temperature, under the influence of heterogeneity. Thus, the free-energy barrier decreases

$$\delta F(T) = \delta E(T) - T\delta S(T) = -\frac{\Delta E_{\mathrm{N}}^{2\neq}}{T} - \frac{\Delta E_{\mathrm{N}}^{2\neq}}{2T} = -\frac{Q^\ddagger(1-Q^\ddagger)\Delta E_{\mathrm{N}}^2}{2T}, \tag{4.22}$$

and the rate in Eq. (4.21) increases as

$$k_f \approx k_{\mathrm{HOMO}}\exp\left(\frac{Q^\ddagger(1-Q^\ddagger)\Delta E_{\mathrm{N}}^2}{2T^2}\right). \tag{4.23}$$

This crude argument yields essentially the same result as the much more detailed functional analysis above [cf. Eq. (4.20)], without the additional factor of $\lambda^\ddagger$. By this argument, even for an initial unperturbed funnel which is fully symmetric (an idealized case where all contacts are equally likely to be formed), introducing arbitrary heterogeneity lowers the folding barrier.

Another argument for the lowering of the barrier makes use of thermodynamic perturbation theory.[86] Consider a Gō model with $M$ contacts, whose configurational states are perturbed in energy by a random contribution $V_c \equiv \delta E_c$ so that the new energy of state $c$ is $E_c = E_c^o + V_c$. Let the native energy be unchanged: $\delta E = 0$ in the native state. Let the fraction of native contacts be $\approx 0$ in the unfolded state for simplicity (the results are not qualitatively changed when this assumption is removed). Then, the change in free energy to second order in $V$ is

$$\delta[F(Q)-F_U(Q\approx 0)]=\delta\Delta F(Q)=\langle V\rangle-\frac{1}{2T}\langle (V-\langle V\rangle)^2\rangle, \tag{4.24}$$

where

$$\langle V\rangle=\frac{1}{Z}\sum_{c\in Q} V_c \exp(-E_c^o/T)=\langle \delta E\rangle_o' \tag{4.25}$$

is calculated by summing over all configurations $c$ having $Q$ native contacts. Now, since the change in a configuration's energy is the sum over perturbations of native contacts made in that state

$$\begin{aligned}\langle \delta E\rangle_o' &= \sum_{c\in Q}{}' \delta E_c \frac{e^{-E_c/T}}{Z} \\ &= \sum_{c\in Q}{}' \sum_{j\in c_N} \delta(j,c)\,\delta\epsilon_j \frac{e^{E_c/T}}{Z}=\sum_{j\in c_N}\langle \delta_j\delta\epsilon_j\rangle \\ &= \sum_{j=1}^{M}\langle \delta_j\rangle\delta\epsilon_j=\sum_{j=1}^{M} Q_j\delta\epsilon_j .\end{aligned} \tag{4.26}$$

The last equality follows from Eq. (2.1). Thus, the first-order change in free energy is simply the sum of the perturbations times the fraction of time those perturbations are felt, as in Eq. (4.8). However, here the first-order term is the sum of a large number of random uncorrelated terms, and so is distributed in a Gaussian-type manner over realizations of the perturbation. The mean of this distribution is zero since the perturbation is randomly made contact to contact

$$\overline{\delta\Delta F}=\sum_i^M \overline{Q_i\delta\epsilon_i}=MQ\,\overline{\delta\epsilon}=0, \tag{4.27}$$

i.e., $\overline{\delta\epsilon}=(1/M)\Sigma_i^M\delta\epsilon_i=0$, because the native energy is unchanged.[104] The standard deviation

$$\sqrt{\overline{(\delta\Delta F)^2}}=\sqrt{MQ(1-Q)b}, \tag{4.28}$$

scales like $\sqrt{N}$ since $M=zN$. Therefore, the first-order term in (4.24) will be $\pm\text{const.}\times N^{1/2}$. Here, we've let the individual contact variance $\overline{\delta\epsilon_i^2}=b^2$. Similar arguments of the effects of heterogeneity on the barrier were considered in Ref. 25.

On the other hand, the second-order term in (4.24) is proportional to $\langle \delta V^2\rangle$ and so scales like $N$, and is always negative. By the reasoning in Eq. (4.26), the average over realizations of native disorder of the thermal fluctuation is

$$\overline{\langle V^2\rangle-\langle V\rangle^2}=\sum_{i,j=1}^{M}\overline{\delta\epsilon_i\delta\epsilon_j}\;\overline{[\langle\delta_i\delta_j\rangle-\langle\delta_i\rangle\langle\delta_j\rangle]}. \tag{4.29}$$

Since the perturbations are independent of each other the cross terms in the sum vanish $\overline{\delta\epsilon_i\delta\epsilon_j}=\overline{\delta\epsilon_i^2}\delta_{ij}=b^2\delta_{ij}$, and

$$\overline{\langle V^2\rangle-\langle V\rangle^2}=\sum_{i=1}^{M} b^2\overline{Q_i(1-Q_i)}, \tag{4.30}$$

where the last equality follows from the fact that the fluctuations of particles obeying Fermi–Dirac statistics [cf. Eq. (3.34)] obey the property $\langle\delta_i^2\rangle-\langle\delta_i\rangle^2=\langle\delta_i\rangle(1-\langle\delta_i\rangle)$. The sum in (4.30) has the form of $M$ positive terms and thus scales extensively ($\sim M$) with the size of the system as opposed to the first-order term. Thus, the free-energy change due to random perturbations in the native energies is negative in the thermodynamic limit. Since native contacts are less formed in the unfolded state than in the transition state, the change in barrier height is also negative in the thermodynamic limit. It is important to note that here the original distribution of energies did not have to be at an optimum. As long as the perturbations were random, the barrier is lowered. Thus, for example if all the $\epsilon_i$ were the same (not the optimal $\epsilon_i^*$ as long as there is a loop length distribution), the barrier would still be lowered after a random perturbation of the native contact energies.

That higher-order terms do not reverse the trend in barrier height can be ensured by the Peierls–Bogoliubov inequality $F\leqslant F_o+\langle V\rangle_o$, where $F_o$ is the free energy in absence of the random component and $V$ is the random part of the Hamiltonian averaged over the unperturbed states, which is just the first-order term in Eq. (4.24). Thus, the transition state free energy (per volume) $F(Q^\dagger)/N$ is always less than the unperturbed free energy $F_o(Q^\dagger)/N$ in the thermodynamic limit, and since $F(0)\cong F_o(0)$ in the unfolded state, the barrier is always lowered.

### B. Including structural heterogeneity and correlations between energetics and structure

The theory also allows us to investigate the effects of native structural variance on the barrier, as well as the correlations between structure and energetics. A perturbation analysis shows that structural variance lowers the barrier, and that entropically likely contacts should be made stronger to lower the barrier. In the model, entropically likely contacts are short-ranged. However, they may occasionally be long-ranged when entropy is more precisely accounted for by accurately accounting for correlations between contacts.

Consider perturbing the free energy of a homogeneous system to second order, with $l_i=\overline{l}$, $\epsilon_i=\overline{\epsilon}$, $Q_i=Q^\ddagger$, by letting $l_i=\overline{l}+\delta l_i$ and $\epsilon_i=\overline{\epsilon}+\delta\epsilon_i$. Then

$$\begin{aligned}&\Delta F^\ddagger\{\overline{\epsilon}+\delta\epsilon_i,\overline{l}+\delta l_i\} \\ &\quad=\Delta F^\ddagger_{\mathrm{MF}}\{\overline{\epsilon},\overline{l}\}+\sum_i\left(\frac{\delta\Delta F^\ddagger}{\delta\epsilon_i}\right)_{\overline{\epsilon},\overline{l}}\delta\epsilon_i+\sum_i\left(\frac{\delta\Delta F^\ddagger}{\delta l_i}\right)_{\overline{\epsilon},\overline{l}}\delta l_i \\ &\qquad+\frac{1}{2!}\sum_{i,j}\left(\frac{\delta^2\Delta F^\ddagger}{\delta\epsilon_i\delta\epsilon_j}\right)_{\overline{\epsilon},\overline{l}}\delta\epsilon_i\delta\epsilon_j \\ &\qquad+\frac{1}{2!}\sum_{i,j}\left(\frac{\delta^2\Delta F^\ddagger}{\delta l_i\delta l_j}\right)_{\overline{\epsilon},\overline{l}}\delta l_i\delta l_j \\ &\qquad+\frac{1}{2!}\sum_{i,j}\left(\frac{\delta^2\Delta F^\ddagger}{\delta l_i\delta\epsilon_j}\right)_{\overline{\epsilon},\overline{l}}\delta l_i\delta\epsilon_j\cdots .\end{aligned} \tag{4.31}$$

The first term in the expansion $\Delta F^\ddagger_{\mathrm{MF}}\{\overline{\epsilon},\overline{l}\}$ is the mean-field free-energy Eq. (3.30). The second term is zero at the extremum where $Q_i=Q^\ddagger$ by Eqs. (4.8), (4.12), and (4.2), and the fourth term is given in Eq. (4.19). The calculation of the third term proceeds along the same lines as the derivation of Eq. (4.8). Like Eq. (4.6), $\delta\Delta F/\delta l_i$ contains a term involving an

explicit derivative of $l_i$, and implicit derivatives which are identically zero. The explicit term itself vanishes when evaluated for homogeneous fields. From Eq. (3.31)

$$\left(\frac{\delta\Delta F^{\ddagger}}{\delta l_i}\right)_{\overline{\epsilon},\overline{l}} = \frac{3}{2}T\left(\frac{Q_i - Q^{\ddagger}}{l_i}\right)_{\overline{\epsilon},\overline{l}} = 0. \tag{4.32}$$

Calculation of the fifth term involves calculating $\delta Q_j/\delta l_i$, which proceeds analogously to the derivation of Eq. (4.18) via (4.15)

$$\frac{\delta Q_j}{\delta l_i} \cong -\delta_{ij}\frac{3}{2}\frac{Q_j(1-Q_j)}{\lambda l_j}, \tag{4.33}$$

which is again diagonal and negative as is Eq. (4.18); raising the energy of a contact or increasing its loop length decreases that contact's probability of formation. From Eqs. (4.32) and (4.33), the fifth and sixth terms in Eq. (4.31) can be calculated, yielding

$$\begin{aligned}\Delta F^{\ddagger}\{\overline{\epsilon}+\delta\epsilon_i, \overline{l}+\delta l_i\} &= \Delta F^{\ddagger 0}\{\overline{\epsilon},\overline{l}\} - M\frac{Q^{\ddagger}(1-Q^{\ddagger})}{2\lambda^{\ddagger}T}\overline{\delta\epsilon^2} \\ &\quad - MT\frac{9}{8}\frac{Q^{\ddagger}(1-Q^{\ddagger})}{\lambda^{\ddagger}}\frac{\overline{\delta l^2}}{\overline{l}^2} - M\frac{3}{4}\frac{Q^{\ddagger}(1-Q^{\ddagger})}{\lambda^{\ddagger}}\frac{\overline{\delta l\,\delta\epsilon}}{\overline{l}}.\end{aligned} \tag{4.34}$$

The second term on the right-hand side of Eq. (4.34) describes the lowering of the barrier with energetic variance, as discussed in the last section. The third term in Eq. (4.34) indicates that structural dispersion also lowers the barrier. The fourth term indicates that the free-energy barrier is additionally lowered in the model when shorter-range contacts become stronger energetically ($\delta l_i<0$ and $\delta\epsilon_i<0$) or longer-range contacts become weaker energetically ($\delta l_i>0$ and $\delta\epsilon_i>0$). This means in general that the free energy is additionally lowered when fluctuations are correlated so as to further increase the variance in contact participations. Note again that all reductions in free energy due to structural and/or energetic heterogeneity are second-order effects, and scale extensively with system size.

To see intuitively how the fourth term in Eq. (4.34) arises, consider taking two contacts $i=1, 2$ within a protein, having formation probabilities $Q_1$, $Q_2$, and making equal and opposite energetic perturbations on them $\delta\epsilon>0$. Now, by Eq. (4.8) the total change in free energy to first order is

$$\delta F \cong -Q_1\delta\epsilon + Q_2\delta\epsilon = -(Q_1-Q_2)\delta\epsilon, \tag{4.35}$$

so if $Q_1>Q_2$ the change in free energy is negative and if $Q_2>Q_1$, $\delta F>0$. Since contacts are *typically* unformed or less formed in the unfolded state, we can say that if $Q_1(Q^{\dagger})>Q_2(Q^{\dagger})$, $\delta\Delta F^{\ddagger}<0$ and *vice versa*.

Since for well-designed two-state folders the rate is controlled most strongly by the free-energy barrier rather than the prefactor, the assertion that heterogeneity in folding increases the rate is then demonstrated. Some obvious caveats include perturbations on a protein not well-designed, or a mutation which anomalously strengthens an off-pathway trap, perturbations of contacts involving residues anomalously formed in the unfolded state, or situations where strengthening one of the contacts lowers the free energy of an on-pathway intermediate; for these exceptional cases the rate-enhancement effect may not be observed.

### C. Dependence of the barrier height on mean loop length (contact order)

Experimental evidence has shown a strong correlation of folding rate with a quantity in our model equal to the mean loop length divided by the total chain length.[35] Since no strong correlation with $N$ is observed, at least for typical protein sizes, we are interested in testing if the barrier height in our model correlates with $\overline{l}$, at fixed $N$.

We seek the change in free energy $\delta F$ upon a change in the quantity $(1/M)\Sigma_i l_i$. This can be found by utilizing the directional derivative [see the Appendix and Eq. (A5)]

$$\frac{\delta F}{\delta\overline{l}} = M\frac{\delta F}{\delta(\Sigma_i l_i)} = \left(\sum_i \hat{\imath}\right)\cdot\left(\sum_j \frac{\delta F}{\delta l_j}\hat{\jmath}\right) = \sum_i \frac{\delta F}{\delta l_i}. \tag{4.36}$$

Using again the analog of Eq. (4.6) that we already used to obtain Eq. (4.32), the total derivative of $F$ with respect to $l_i$ is equivalent to the partial derivative. The free energy $F$ depends on $l_i$ explicitly only through the bond entropy Eq. (3.25), which is composed of a mean-field term depending on the sum $\overline{l}$ plus a fluctuation term, Eqs. (3.26) and (3.27). Noting that

$$\frac{\partial\mathcal{S}_{\mathrm{MF}}(Q,\overline{l})}{\partial l_i} = \frac{1}{M}\frac{\partial\mathcal{S}_{\mathrm{MF}}(Q,\overline{l})}{\partial\overline{l}},$$

we obtain

$$\begin{aligned}\frac{\partial F}{\partial\overline{l}} &= -T\frac{\partial\mathcal{S}_{\mathrm{BOND}}}{\partial\overline{l}} \\ &= \frac{3}{2}\frac{MT}{(\overline{l}-1)^2}[\ln(1+(\overline{l}-1)Q) - Q\ln\overline{l}] \\ &\quad + \frac{3}{2}MT\left\langle\frac{\delta Q}{l}\right\rangle.\end{aligned} \tag{4.37}$$

The first term in expression (4.37) is always positive for $Q>0$. The second term weights loops with smaller $l_i$ more heavily, and for these loops $\delta Q>0$, so the second term is always positive when entropic effects are considered alone. The native energies would have to be specially tuned to change the sign of this term. Moreover, the whole expression is zero when $Q=0$, so we conclude that the effect of increasing the mean loop length is to increase the barrier height $\Delta F^{\ddagger}$. This effect is illustrated in Fig. 6 for the simple case where $l_i=\overline{l}$, i.e., where the second term in (4.37) is zero. This is a lower limit to the actual increase in barrier.

As Eq. (4.37) implies, the change in barrier height with mean loop length is an entropic effect; proteins with native structures having larger mean loop length have lower entropy near the transition state. Another perhaps simpler way to see this is to note that the entropy of loop closure must become

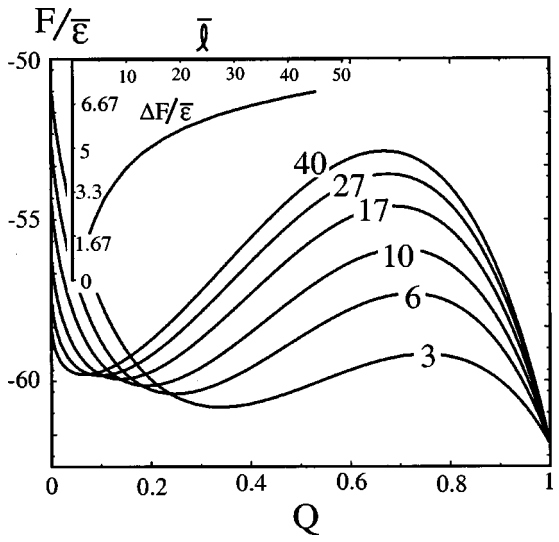


FIG. 6. Dependence of the free-energy profile $F(Q)$ at $T_F$ on the mean loop length $\overline{l}$, for the analytic model with length $N=50$, $l_i=\overline{l}$, and $\epsilon_i=\overline{\epsilon}$ [Eqs. (3.29) and (3.30)]. $\overline{l}$ labels each curve. The barrier undergoes an increase that is stronger initially. The inset plots the barrier height as a function of $\overline{l}$, in units of $\overline{\epsilon}$. The trend in barrier height with $\overline{l}$ shown here is a lower limit to the full theoretical dependence given in Eq. (4.37).

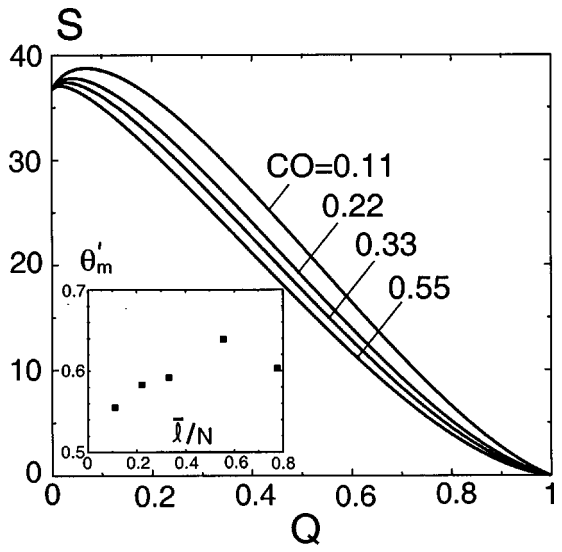


FIG. 7. Entropy vs $Q$ for $\epsilon_i=\overline{\epsilon}$ and $l_i=\overline{l}$, for various $\overline{l}$. The contact order $\equiv\overline{l}/N$ ($N=27$ here) labels each curve (Ref. 105). As $\overline{l}$ increases, more entropy is lost initially, leading to a larger free-energy barrier and correspondingly slower folding rate. (Inset): The model shows a weak increasing dependence of $\theta'_m$ value with contact order, defined here as the relative degree of partial order at the barrier peak: $\theta'_m \equiv (Q^\dagger - Q_U)/(1-Q_U)$. The trends seen here are again lower limits to the full dependence on $\overline{l}$ given in Eq. (4.37); we illustrate just the mean-field term here.

larger (more negative) as the loop length for that contact is increased. From Eqs. (3.18) and (3.19) and setting $l_i=\overline{l}$ for purposes of illustration

$$\frac{\partial s_i}{\partial \overline{l}} \approx -\frac{1-Q}{\overline{l}(1+(\overline{l}-1)Q)} < 0. \tag{4.38}$$

Therefore, more entropy is lost in contact formation for structures with larger mean loop length. Furthermore, since

$$\frac{\partial^2 s_i}{\partial Q \partial \overline{l}} \approx \frac{1}{(1+(\overline{l}-1)Q)^2} > 0, \tag{4.39}$$

this effect is largest at low degrees of nativeness [e.g., from Eq. (4.38) at $Q=0$, $\partial s_i/\partial \overline{l} \approx -1/\overline{l}$ while at $Q=1$ $\partial s_i/\partial \overline{l} \approx 0$]: the entropy becomes more of a convex down function as $\overline{l}$ is increased; see Fig. 7. Since the free-energy barrier arises from the incomplete cancellation of entropy and energy (which is independent of $\overline{l}$) as $Q$ increases, a more convex down entropy indicates a larger barrier height.

### D. Dependence of barrier heights and rates on structural variance

By Eq. (4.34), if we let $\epsilon_i=\overline{\epsilon}$ and fix $\overline{l}$, the folding barrier is lower for structures with larger variance in loop energies $\overline{\delta l^2}$. For proteins sufficiently well-designed that the folding rate $k_F$ near the transition temperature is governed by the free-energy barrier as in Eq. (1.1), then

$$\ln \frac{k_F(\overline{\delta l^2})}{k_F(0)} \approx M Q^\ddagger \frac{\overline{\delta l^2}}{\overline{l^2}}, \tag{4.40}$$

where we have also neglected changes in the folding transition temperature, since accounting for this is a higher-order effect. We have also let $\lambda^\ddagger \approx 1-Q^\ddagger$, since $\alpha$ in Eq. (3.11b) is approximately 1.[49,52] Most importantly, the perturbation result neglects changes in the unfolded free energy on structural variance, as well as changes in the amount of native structure in the unfolded state. These reduce the trend on the rate due to structural variance. In general, we should use

$$\ln \frac{k_F(\overline{\delta l^2})}{k_F(0)} \cong \frac{\Delta F^\ddagger(0)}{T_F(0)} - \frac{\Delta F^\ddagger(\overline{\delta l^2})}{T_F(\overline{\delta l^2})}, \tag{4.41}$$

for the log ratio of rates. The barrier height is then obtained from Eqs. (3.29) and (3.34). It is seen in Fig. 8 that there is a significant increase in folding rate for structures having larger variance in loop lengths. Structural variance is generated here for a system with parameters characterizing the system in Fig. 1,[105] but the loop lengths are given by

$$l_i = \overline{l} + \alpha(l_i^o - \overline{l}), \tag{4.42}$$

where $l_i^o$ is taken from the full loop length distribution. As $\alpha$ varies from zero to 1, the mean loop length $\overline{l}$ remains unchanged ($\overline{l} \cong 9.14$), but the structural variance $\overline{\delta l^2}$ increases (see Fig. 8).

### E. Measures of routing

Since the free-energy barrier is maximized for a uniform funnel folding mechanism [Eq. (4.18)], we expect the barrier height to be a decreasing function of the dispersion in $Q_i$

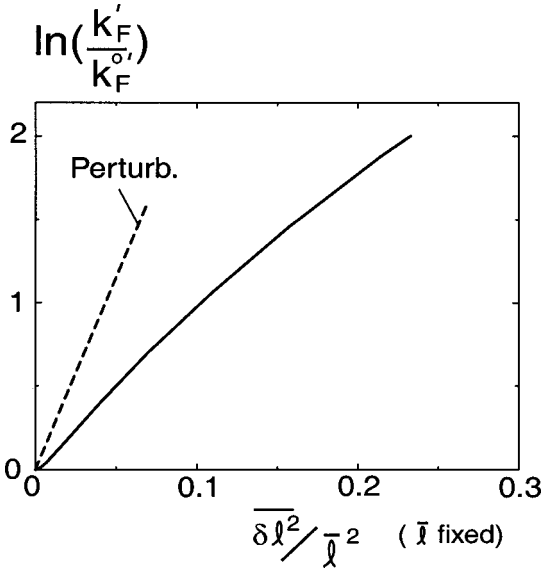


FIG. 8. Log of the ratio of rates given by Eq. (4.41) as a function of structural variance $\overline{\delta l^2}$ at fixed $\bar{l}$, obtained by following the recipe of Eq. (4.42). (Dashed): Approximate perturbation result of Eq. (4.40). (Solid): Full nonperturbative result using Eqs. (3.29) and (3.34), which accounts for changes in the unfolded free energy with increasing variance. The barrier is calculated at $T_F$, which changes only mildly with $\overline{\delta l^2}$ until the barrier height approaches zero at $\overline{\delta l^2}/\bar{l}^2 \approx 0.25$.

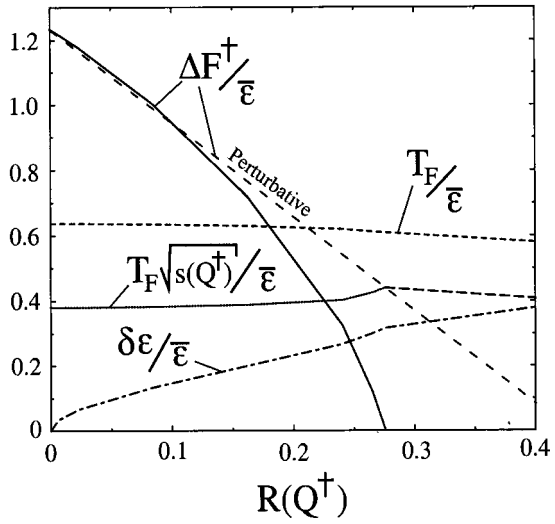


FIG. 9. Free-energy barrier at the transition temperature $T_F$ in units of $\overline{\epsilon}$, vs the route measure at the barrier peak $\mathcal{R}(Q^{\ddagger})$. (Solid line): Theoretical result with parameters modeling a lattice protein (Ref. 105). (Long dashed): perturbative result in Eq. (4.45). (Short dashed): folding transition temperature. Also shown are the folding temperature weighted by the entropy at the barrier peak, and standard deviation in energies in units of the mean native energy (see the text).

values at the barrier peak $\overline{\delta Q^2}(Q^{\ddagger}) = \langle (Q_i - Q^{\ddagger})^2 \rangle$. Let us introduce a measure of "routing" $\mathcal{R}(Q^{\ddagger})$ through the bottleneck by the function

$$\mathcal{R}(Q) = \frac{\langle \delta Q^2 \rangle}{\langle \delta Q^2 \rangle_{\mathrm{MAX}}} = \frac{\langle \delta Q^2 \rangle}{Q(1-Q)}. \tag{4.43}$$

The denominator is the most route-like the system can get at $Q$, i.e., if $MQ$ contacts were made with probability 1 and $M-MQ$ contacts were made with probability 0, then $\langle (Q_i - Q)^2 \rangle = (1/M)(MQ(1-Q)^2 + (M-MQ)Q^2) = Q(1-Q)$. Thus, $\mathcal{R}(Q)$ is between 0 and 1. $\mathcal{R}(Q)$ is proportional to the lowest-order correction to the route entropy (3.11a) when fluctuations $\delta Q$ are present

$$\mathcal{S}_{\mathrm{ROUTE}}(\{Q + \delta Q_i\}) \cong \mathcal{S}^{o}_{\mathrm{ROUTE}} - \frac{M\lambda}{2}\mathcal{R}(Q). \tag{4.44}$$

In the (nonperturbative) limit $\mathcal{R}(Q) = 1$, $\mathcal{S}_{\mathrm{ROUTE}} = 0$, and only one route to the native state is allowed, i.e., since all $Q_i$ are only zero or 1 at any degree of nativeness, each successive bond added at that degree of nativeness must always be the same one. This was the pathway-like folding mechanism originally proposed by Levinthal.[106]

Using Eq. (4.18) we can relate the fluctuations in optimal energies $\delta\epsilon_i$ in terms of fluctuations from the uniform contact probabilities $\delta Q_i$ as $\delta\epsilon_i = -\lambda T \delta Q_i / Q^{\ddagger}(1-Q^{\ddagger})$, and then substitute this along with (4.18) into Eq. (4.3) to obtain the decrease in barrier height with route measure

$$\delta\Delta F^{\ddagger} \cong -M\frac{\lambda^{\ddagger} T}{2}\frac{\overline{\delta Q^2}}{Q^{\ddagger}(1-Q^{\ddagger})} = -M\frac{\lambda^{\ddagger} T}{2}\mathcal{R}(Q^{\ddagger}). \tag{4.45}$$

Again, the reduction in the barrier height due to ordering heterogeneity scales extensively with system size. A dispersion in contact participations $\overline{\delta Q^2} = 0.05$, which is about 20% of the maximal dispersion ($\approx 1/4$, taking $Q^{\ddagger} \approx 1/2$), lowers the barrier by about $0.1 N k_B T$ or about $5 k_B T$ for a chain length $N \approx 50$, believed to model a protein with $\approx 100aa$.[31] We should note here that renormalizing real amino acids into coarse-grained monomers may underestimate the heterogeneity effect, because small-scale free-energy fluctuations do not average out upon coarse graining, but will still add up extensively. Plots of the route measure as a function of $Q$ for the various possible folding scenarios were given in Ref. 49.

Figure 9 shows the barrier height at the folding transition temperature $T_F$ in units of $\overline{\epsilon}$, vs the route measure at the barrier peak $\mathcal{R}(Q^{\ddagger})$. There is a monotonically decreasing trend in the barrier height away from the uniformly folding state governed by Eq. (3.30), when routing is increased from zero by randomly perturbing the native energies. The solid line in Fig. 9 is the theoretical result for a model parametrizing a fast-folding 27-mer model[105] (see Refs. 49 and 52 for further comparison). The short dashed line is the perturbation result for this model from Eq. (4.45), which agrees reasonably well with the full nonperturbative result for small $\mathcal{R}$. Some discrepancy is present because routing may affect the free energy of the unfolded state to a smaller extent, i.e., as local contacts are made stronger they are more likely to be present in the unfolded state. A moderate to large variance in energies is required to eliminate the barrier, when energetic perturbations are made randomly as shown here. When energies are allowed to correlate with native topology as in Eq. (4.34), a significantly smaller variance is required to eliminate the barrier.[49] The folding temperature $T_F$ is itself weakly dependent on $\mathcal{R}(Q^{\ddagger})$, for small to moderate degrees of routing. Another measure of the degree of self-averaging weights the folding temperature by the entropy at the barrier peak,

which is itself a function of the degree of routing. However, because polymer halo entropy increases compensate for route entropy decreases as $\mathcal{R}(Q^{\ddagger})$ is increased from zero, this measure remains roughly constant over the full range of barrier heights (see Fig. 9).

## V. SUMMARY AND CONCLUSIONS

In this paper we have introduced a general theoretical framework to study the effects of heterogeneity on the thermodynamics and mechanism of protein folding. We have explored in minimally frustrated sequences how folding is affected by heterogeneity in native contact energies, as well as the entropic heterogeneity inherent in folding to a specific three-dimensional native structure. The general method we utilized here should be amenable to systematic refinement, and should be sufficiently accurate to compare with experimental results.

Specifically, we found that heterogeneity in the folding mechanism, i.e., in the native contact probabilities, always lowers the folding free-energy barrier, as long as $T_F/T_G > 1$. This heterogeneity may arise from variations in native contact energies, or variations in native loop lengths. When the energy landscape is funneled overall, the barrier can still be sensitive to the details of the energetics and entropics. For sufficiently well-designed proteins it can be shown that the corresponding rate also increases as heterogeneity in folding mechanism increases.[52] The effects of heterogeneity on barriers and rates are stronger than the effects on transition temperature, so that barriers may be reduced while kinetic prefactors are not strongly affected. We investigated the effects on the folding barrier due to correlations between energetics and topology, and found that for well-designed proteins the rate may be increased by making initially likely contacts stronger while making unlikely contacts weaker. Thus, overall stability is conserved, but the energetic distribution is coupled to the native structure.

Associating a decrease in thermodynamic barrier with an increase in rate assumes that not too much dynamic information is lost when one projects the free-energy landscape onto one reaction coordinate such as $Q$. This is a good approximation for proteins with a single dominant time scale governing folding.[107] Even for proteins with several time scales undergoing kinetic partitioning,[108] the correlation between barriers and rates should be a good one so long as the protein is minimally frustrated. As long as the heterogeneity is in a regime where the global properties of the folding funnel do not change, i.e., $T_F/T_G$ varying slowly and sufficiently larger than 1, lowering the free-energy barrier is essentially equivalent to increasing the rate. However, one has to be careful that the folding heterogeneity is not so large that this regime breaks down. In lattice simulations to well-designed structures it has been observed that $\phi$ values correlate with $Q_i$ values as well as any other reaction coordinate currently proposed;[101] for example, probability to fold before unfolding.[75] However, it is still possible that some proteins may be poorly designed, or have very specific folding nuclei due to their native structure.

Residues in proximity are assumed to be in contact energetically, and a pair contact Hamiltonian was used.[109] If many-body forces are not too large the barrier may be reduced to zero, either by adding random native heterogeneity or by correlating native energy to native structure so that more probable contacts are stronger, as in Sec. IV B. Tuning the energies further so that probable contacts have even lower energy (or allowing native energies to have a very large variance) eventually induces the system to take a single route or very few folding routes at the transition temperature. A large dispersion of energies is required to achieve this, and in this regime the folding temperature drops well below the glass temperature range, where folding rates are extremely slow. The funnel picture, with different structural details, is valid for the above wide range of native contact energy distributions.

The formalism we developed here allowed us to treat both the energetics and the entropics involved in folding. We derived approximate expressions for the conformational entropy functional for a well-designed protein. We generalized the entropy of native core placement (the mixing entropy) used previously in models of folding[87,88] to account for the effects of chain connectivity; for a highly constrained chain, many contact patterns degenerate to essentially the same conformation. In Sec. III B 2 we derived a general condition for the conformational entropy to be a state function, viz. Eq. (3.14). A Hartree-style approximation was taken to account for the entropy loss of loop closure in the presence of other contacts already formed. Equation (3.25) gives the conformational entropy loss given a distribution of native contact lengths $\{l_i\}$. When each $l_i \to \overline{l}$, the expression reduces to Eq. (3.26), which is the entropy loss for a finite system with mean return length $\overline{l}$ for all contacts. When $\overline{l} \to \infty$, (3.26) further reduces to Eq. (3.28), which is the entropy loss for a polymer system in the Flory mean-field theory.[91] Other treatments for the entropics are possible within the general framework we developed, for example a formulation of the entropy within the capillarity approximation, or even a computationally derived entropy functional taken from simulation data.

Several experiments support results from our theory. Enhancement of folding rates by weighting entropically likely contacts has been observed in *Escherichia coli Che Y*.[110] Depending on the variance of native interactions and how native interaction strength correlates with the entropic likelihood of contact formation, sequences may be designed to fold both faster or slower to the same structure as a wild-type sequence, even at the same overall stability. Enhancement or suppression of folding rate to a given structure due to changes in sequence are modeled in our theory through changes in native interactions, which induce significant changes in the rate-governing free-energy landscape of a well-designed protein. A minimally frustrated sequence may fold to a given native structure by a variety of folding mechanisms, including both on-and off-pathway intermediates. Thus, for example folding in Im 7 and Im 9 may likely initiate from different places within the native structure depending on the distribution of native stabilizing interactions.[16] Folding in the IgG binding domain of protein L may tend to initiate from a specific region of higher local stability, indiscernible from the apparently symmetric native

structure;[111] contact formation probability at the transition state depends on both energy and entropy, as expressed in Eq. (3.34).

For a large range of native energy distributions, barrier heights, and corresponding rates, a funneled folding mechanism is preserved. Folding rates in mutant proteins that exceed those of the wild type have been receiving much interest in recent experiments;[17,110,112–114] here, we see how these effects can be understood by applying general principles of the energy landscape. Folding barriers in the theory were seen to decrease with the increasing variance in contact formation probability, a thermodynamic quantity closely related to the dispersion in experimental $\phi$ values. We believe that testing this theory should be quite possible with the experimental techniques utilizing point mutations which are available today. The observed trend of reduced rate with larger contact order[35] is also seen in the theory (see Fig. 6); however, the trend seems to be not as great, indicating that cooperative interactions may be playing a role. Additionally, for fixed contact order, folding rate was shown to increase with larger variance in the contact lengths which constitute the native structure.

Fluctuations in rate due to weakening or strengthening specific non-native kinetic traps or generally changing non-native interaction strength are not treated in detail by the theory, and are an interesting topic of future research.

It is important to note that the enhancements or reductions in rate we have explored here are mild compared to the enhancement by minimal frustration (funneling the landscape): the fine tuning of rates may be a phenomenon manifested by *in vitro* or *in machina* evolution, rather than *in vivo* evolution. Nevertheless, folding heterogeneity may become an important factor for larger proteins, where, e.g., destabilizing partially native intermediates may decrease the overall rate but prevent aggregation. For some proteins such as S6, rate measurements imply that folding is more cooperative for the wild type than for several permutants;[115] however, the trend in rate can be explained largely by changes in contact order.[35] On the other hand, it was noticed that for the permutants, heterogeneity in the transition state had increased as well. Transition state drift measurements imply that folding is more cooperative for wild-type chymotrypsin inhibitor than for several mutants.[116] The suggestion that wild-type proteins fold more cooperatively implies that evolutionary selection for either reduced conformational fluctuations from the native state or reduced Boltzmann weight of partially structured conformations may have been more important than selection for the mild rate enhancements due to heterogeneous folding, at least in some proteins. It is also possible that selection for native stability induces *en passant* a larger folding barrier when conditions are adjusted so the wild-type protein has the same stability as the mutant. However, this issue of what evolution chose to select for does not bear upon the statistical mechanical conclusions we found here. Adjusting the backbone rigidity or the nonadditivity of interactions[24,71,84] can also modify the barrier height, possibly as much as the effects we are considering here. There may also be functional reasons for nonuniform folding—malleability or rigidity requirements of the active site may inhibit or enhance its tendency to order.

The notion expounded here that rates increase with heterogeneity at little expense to transition temperature contrasts with the view that nonuniform folding in real proteins exists merely as a residual signature of incomplete evolution to a uniformly folding protein, if rate is exclusively selected for. Moreover, the phenomenon that random fluctuations in native contact energies contribute extensively to the free-energy landscape indicates that the prediction of numerical values for folding rates and mechanisms from approximate energy functions may be even more difficult than originally suspected, i.e., even if systematic error in the calculation of potentials is eliminated, $\mathcal{O}(\mathcal{N})$ corrections may still remain.

The amount of route narrowness in folding was introduced as a thermodynamic measure through the mean-square fluctuations in a local order parameter. The route measure may be useful in quantifying the natural kinetic accessibility of various structures. While structural heterogeneity is essentially always present, the flexibility inherent in the number of letters of the sequence code limits the amount of native energetic heterogeneity possible. However, some sequence flexibility is in fact required for funnel topographies[117] and so is probably present, at least to a limited degree.

We have seen here how a very general theoretical framework can be introduced to explain and understand the effects of heterogeneity in native stabilizing interactions and heterogeneity in structural topology on such quantities as folding rates, transition temperatures, and the degree of routing in the funnel folding mechanism. Such a theory should be a useful guide in interpreting and predicting future experimental results on many fast-folding proteins.

## ACKNOWLEDGMENTS

The authors thank Peter Wolynes, Hugh Nymeyer, and Cecilia Clementi for their generous and insightful discussions. This work was supported by NSF Bio-Informatics Fellowship No. DBI9974199 and NSF Grant No. MCB0084797.

## APPENDIX: INTERPRETING THE LAGRANGE MULTIPLIER AND DIRECTIONAL DERIVATIVE

Consider the free energy of Eq. (3.8) as the integral over a semilocal free-energy density $F(\{Q_i\})=\Sigma_i f_i(Q_i,Q)=\Sigma_i f_i(Q_i,\Sigma_j Q_j)$. Taking the differential of a new thermodynamic function $G=F+\mu\Sigma_i Q_i$

$$\delta G=\sum_i \left[\left(\frac{\partial f_i}{\partial Q_i}\right)_\mu+\mu\right]\delta Q_i+\left[\sum_j Q_j\right]d\mu, \tag{A1}$$

and demanding that $\partial G/\partial Q_j=0$ for all $j$ Legendre transforms to a new variable $\mu$, with $\partial G/\partial\mu=MQ$. This is equivalent to minimizing the free energy subject to the constraint of fixed $Q$. The equation $\partial G/\partial Q_j=0$ means that

$$\frac{\partial f_i}{\partial Q_i}=-\mu \tag{A2}$$

for all $i$, which enforces Eq. (3.34) for each $Q_i$. The Lagrange multiplier $\mu$ is interpreted as the force corresponding to the potential $F(Q)$

$$\mu = -\frac{1}{M}\frac{\partial F(\{Q_i\})}{\partial Q}, \tag{A3}$$

by the following arguments. From Eq. (A1) $(\partial G/\partial Q_i)_\mu = 0$ is equivalent to $\partial F/\partial Q_i + \mu = 0$, or

$$\mu = -\frac{\partial F}{\partial Q_i} \text{ for any } i, \tag{A4}$$

therefore, $\mu = -(\partial Q/\partial Q_i)(\partial F/\partial Q) = -(1/M)(\partial F/\partial Q)$. Since the changes with respect to the local order parameter of all the local free-energy terms are the same number $\mu$ [Eq. (A2)], this number equals the change in the sum ($F$) with respect to the change in the sum of the $Q_i(MQ)$ [Eq. (A3)].

Another way to see Eq. (A3) directly is to consider $\partial/\partial(MQ) = \partial/\partial(\Sigma_{i=1}^{M} Q_i)$ as the directional derivative $D_{\mathbf{u}}F$ of $F$ in an $M$-dimensional space along the direction $\nabla Q = \Sigma_i \hat{\imath}$ with $\hat{\imath}$ a unit vector along the $i$th axis, defined by the $i$th contact. So

$$\begin{aligned}\frac{\partial F}{\partial(\Sigma_{i=1}^{M} Q_i)} &= \frac{1}{|\nabla Q|} D_{\mathbf{u}} F \\ &= \frac{1}{\sqrt{M}} \frac{\nabla Q}{|\nabla Q|} \cdot \nabla F(\{Q_i\}) \\ &= \frac{1}{M}\left(\sum_i \hat{\imath}\right) \cdot \sum_j \frac{\partial F}{\partial Q_j}\hat{\jmath} = -\frac{\mu}{M}\sum_{ij} \hat{\imath}\cdot\hat{\jmath} = -\mu.\end{aligned} \tag{A5}$$

For the two-state potentials considered here, $\mu$ has two roots which give the positions of the barrier peak and equilibrium unfolded state (where the local force is zero).


[1] P. G. Wolynes, in *Spin Glasses and Biology*, edited by D. L. Stein (World Scientific, Singapore, 1992), pp. 225–259.
[2] J. D. Bryngelson, J. N. Onuchic, N. D. Socci, and P. G. Wolynes, Proteins **21**, 167 (1995).
[3] K. A. Dill, S. Bromberg, K. Yue, K. M. Fiebig, D. P. Yec, P. D. Thomas, and H. S. Chan, Protein Sci. **4**, 561 (1995).
[4] K. D. Ball, R. S. Berry, R. E. Kunz, F. Y. Li, A. A. Proykova, and D. J. Wales, Science **271**, 963 (1996).
[5] K. A. Dill and H. S. Chan, Nat. Struct. Biol. **4**, 10 (1997).
[6] T. Veitshans, D. Klimov, and D. Thirumalai, Folding Des. **2**, 1 (1997).
[7] J. N. Onuchic, Z. Luthey-Schulten, and P. G. Wolynes, Annu. Rev. Phys. Chem. **48**, 545 (1997).
[8] V. S. Pande, A. Y. Grosberg, and T. Tanaka, Biophys. J. **73**, 3192 (1997).
[9] C. M. Dobson, A. Sali, and M. Karplus, Angew. Chem. Int. Ed. Engl. **37**, 868 (1998).
[10] T. Garel, H. Orland, and E. Pitard, in *Spin Glasses and Random Fields*, edited by A. P. Young (World Scientific, River Edge, NJ, 1998).
[11] C. L. Brooks, M. Gruebele, J. N. Onuchic, and P. G. Wolynes, Proc. Natl. Acad. Sci. U.S.A. **95**, 11037 (1998).
[12] A. R. Fersht, *Structure and Mechanism in Protein Science*, 1st ed. (Freeman, New York, 1999).
[13] M. Gruebele, Annu. Rev. Phys. Chem. **50**, 485 (1999).
[14] D. J. Wales and H. A. Scheraga, Science **285**, 1368 (1999).
[15] J. N. Onuchic, H. Nymeyer, A. E. Garcia, J. Chahine, and N. D. Socci, Adv. Protein Chem. **53**, 87 (2000).
[16] N. Ferguson, A. P. Capaldi, R. James, C. Kleanthous, and S. E. Radford, J. Mol. Biol. **286**, 1597 (1999).
[17] D. E. Kim, H. Gu, and D. Baker, Proc. Natl. Acad. Sci. U.S.A. **95**, 4982 (1998).
[18] P. M. Dalessio and I. J. Ropson, Biochemistry **39**, 860 (2000).
[19] V. I. Abkevich, A. M. Gutin, and E. I. Shakhnovich, Biochemistry **33**, 10026 (1994).
[20] J. N. Onuchic, N. D. Socci, Z. Luthey-Schulten, and P. G. Wolynes, Folding Des. **1**, 441 (1996).
[21] D. K. Klimov and D. Thirumalai, J. Mol. Biol. **282**, 471 (1998).
[22] L. Li, L. A. Mirny, and E. I. Shakhnovich, Nat. Struct. Biol. **7**, 336 (2000).
[23] J. D. Bryngelson and P. G. Wolynes, J. Phys. Chem. **93**, 6902 (1989).
[24] S. S. Plotkin, J. Wang, and P. G. Wolynes, J. Chem. Phys. **106**, 2932 (1997).
[25] P. G. Wolynes, Proc. Natl. Acad. Sci. U.S.A. **94**, 6170 (1997).
[26] A. V. Finkelstein and A. Y. Badretdinov, Folding Des. **2**, 115 (1997).
[27] J. D. Bryngelson and P. G. Wolynes, Proc. Natl. Acad. Sci. U.S.A. **84**, 7524 (1987).
[28] R. A. Goldstein, Z. A. Luthey-Schulten, and P. G. Wolynes, Proc. Natl. Acad. Sci. U.S.A. **89**, 4918 (1992).
[29] P. E. Leopold, M. Montal, and J. N. Onuchic, Proc. Natl. Acad. Sci. U.S.A. **89**, 8721 (1992).
[30] E. I. Shakhnovich and A. M. Gutin, Proc. Natl. Acad. Sci. U.S.A. **90**, 7195 (1993).
[31] J. N. Onuchic, P. G. Wolynes, Z. Luthey-Schulten, and N. D. Socci, Proc. Natl. Acad. Sci. U.S.A. **92**, 3626 (1995).
[32] E. Bornberg-Bauer and H. S. Chan, Proc. Natl. Acad. Sci. U.S.A. **96**, 10689 (1999).
[33] N. E. G. Buchler and R. A. Goldstein, J. Chem. Phys. **111**, 6599 (1999).
[34] By fluctuations we mean variations or heterogeneity in a given quantity. Throughout the paper we will freely switch between the terminologies.
[35] K. W. Plaxco, K. T. Simons, and D. Baker, J. Mol. Biol. **277**, 985 (1998).
[36] V. Munoz and W. A. Eaton, Proc. Natl. Acad. Sci. U.S.A. **96**, 11311 (1999).
[37] A. R. Fersht, Proc. Natl. Acad. Sci. U.S.A. **97**, 1525 (2000).
[38] E. Alm and D. Baker, Proc. Natl. Acad. Sci. U.S.A. **96**, 11305 (1999).
[39] B. A. Shoemaker, J. Wang, and P. G. Wolynes, J. Mol. Biol. **287**, 675 (1999).
[40] O. V. Galzitskaya and A. V. Finkelstein, Proc. Natl. Acad. Sci. U.S.A. **96**, 11299 (1999).
[41] J. E. Shea, J. N. Onuchic, and C. L. Brooks, Proc. Natl. Acad. Sci. U.S.A. **96**, 12512 (1999).
[42] D. S. Riddle, V. P. Grantcharova, J. V. Santiago, E. Alm, I. Ruczinski, and D. Baker, Nat. Struct. Biol. **11**, 1016 (1999).
[43] R. Du, V. S. Pande, A. Yu. Grosberg, T. Tanaka, and E. S. Shakhnovich, J. Chem. Phys. **111**, 10375 (1999).
[44] C. Micheletti, J. R. Banavar, A. Maritan, and F. Seno, Phys. Rev. Lett. **82**, 3372 (1999).
[45] C. Clementi, H. Nymeyer, and J. N. Onuchic, J. Mol. Biol. **298**, 937 (2000).
[46] C. Clementi, P. A. Jennings, and J. N. Onuchic, Proc. Natl. Acad. Sci. U.S.A. **97**, 5871 (2000).
[47] D. M. Taverna and R. A. Goldstein, Biopolymers **53**, 1 (2000).
[48] A. Maritan, C. Micheletti, A. Trovato, and J. R. Banavar, Nature (London) **406**, 287 (2000).
[49] S. S. Plotkin and J. N. Onuchic, Proc. Natl. Acad. Sci. U.S.A. **97**, 6509 (2000).
[50] B. A. Shoemaker, J. Wang, and P. G. Wolynes, Proc. Natl. Acad. Sci. U.S.A. **94**, 777 (1997).
[51] B. A. Shoemaker and P. G. Wolynes, J. Mol. Biol. **287**, 657 (1999).
[52] S. S. Plotkin, C. Clementi, and J. N. Onuchic (unpublished).
[53] A. M. Gutin, V. I. Abkevich, and E. I. Shakhnovich, Proc. Natl. Acad. Sci. U.S.A. **92**, 1282 (1995).
[54] S. A. Radford, C. M. Dobson, and P. A. Evans, Nature (London) **358**, 302 (1992).
[55] Y. Bai, T. R. Sosnick, L. Mayne, and S. W. Englander, Science **269**, 192 (1995).
[56] E. M. Boczko and C. L. Brooks, Science **269**, 393 (1995).
[57] T. Lazaridis and M. Karplus, Science **278**, 1928 (1997).
[58] F. B. Sheinerman and C. L. Brooks, Proc. Natl. Acad. Sci. U.S.A. **95**, 1562 (1998).
[59] A. R. Fersht, A. Matouschek, and L. Serrano, J. Mol. Biol. **224**, 771 (1992).
[60] Y. Ueda, H. Taketomi, and N. Gō, Int. J. Pept. Protein Res. **7**, 445 (1975).
[61] N. Gō and H. Abe, Biopolymers **20**, 991 (1981).
[62] H. Abe and N. Gō, Biopolymers **20**, 1013 (1981).
[63] A. Horovitz and A. Fersht, J. Mol. Biol. **224**, 733 (1992).
[64] M.-H. Hao and H. Scheraga, Physica A **244**, 124 (1997).

[65] J. M. Sorenson and T. Head-Gordon, Folding Des. **3**, 523 (1998).
[66] D. K. Klimov and D. Thirumalai, Folding Des. **3**, 127 (1998).
[67] K. Lum, D. Chandler, and J. D. Weeks, J. Phys. Chem. **103**, 4570 (1999).
[68] S. Takada, Z. Luthey-Schulten, and P. G. Wolynes, J. Chem. Phys. **110**, 11616 (1999).
[69] R. B. Prince, J. G. Saven, P. G. Wolynes, and J. S. Moore, J. Am. Chem. Soc. **121**, 3114 (1999).
[70] A. Kolinski, W. Galazka, and J. Skolnick, Proteins: Struct., Funct., Genet. **26**, 271 (1996).
[71] M. P. Eastwood and P. G. Wolynes, Proteins **30**, 215 (2001).
[72] The native backbone topology is more precisely specified by a vector parametrized by the arc length along the polymer chain, $\mathbf{r}(s)$, but it is difficult to apply the formalism starting from this description.
[73] J. F. Douglas and T. Ishinabe, Phys. Rev. E **51**, 1791 (1995).
[74] J. J. Portman, S. Takada, and P. G. Wolynes, Phys. Rev. Lett. **81**, 5237 (1998).
[75] R. Du, V. S. Pande, A. Yu. Grosberg, T. Tanaka, and E. S. Shakhnovich, J. Chem. Phys. **108**, 334 (1998).
[76] J. K. Percus, in *The Liquid State of Matter: Fluids, Simple and Complex*, edited by E. Montroll and J. Lebowitz (North-Holland, Amsterdam, 1982).
[77] R. Evans, in *Fundamentals of Inhomogeneous Fluids*, edited by D. Henderson (Dekker, New York, 1992).
[78] J. D. Gunton, M. S. Miguel, and P. S. Sahni, in *Phase Transitions and Critical Phenomena*, edited by C. Domb and J. L. Lebowitz (Academic, New York, 1983), Vol. 8, pp. 267–466.
[79] H. G. Bohr and P. G. Wolynes, Phys. Rev. A **46**, 5242 (1992).
[80] We will generally set Boltzmann's constant $k_B=1$ in this paper, so temperatures have units of energy, and entropies are in units of $k_B$.
[81] Later in the paper we will assume all quantities are thermally equilibrated, and the averages will indicate sums over native contacts, e.g., $Q=\langle Q_i\rangle$. The meaning should be clear from the context.
[82] For a Gō-type set of interactions, collapse and folding occur simultaneously. $\overline{E}$ in Eq. (3.8) can then be set to zero since all energetic contributions $\Sigma_i Q_i\epsilon_i$ are from native contacts. At the other extreme, if there is no change in density with folding and the total number of contacts of any kind is a constant, the term $\Sigma_i Q_i\epsilon_i$ can be interpreted as the *extra* energy native contacts get. Then $\overline{E}$ is a constant, which again has no effect on the free energy. In an intermediate regime there is some non-native density coupling to progress along the folding reaction coordinate, when the packing fraction $c$ is a function of $Q$ (Refs. 24, 119).
[83] We note in passing that for the ensemble of sequences with only overall stability $\Sigma_i\epsilon_i=E_N$ specified, rather than the whole distribution $\{\epsilon_i\}$ as in Eq. (3.8) above, the non-native ruggedness decreases with $Q$ as $\sim(1-Q^2)$ (Ref. 24), rather than as $(1-Q)$ as above. This results from averaging over the native coupling energies under the constraint $\Sigma_i\epsilon_i=E_N$.
[84] A. Kolinski, A. Godzik, and J. Skolnick, J. Chem. Phys. **98**, 7420 (1993).
[85] M. Vendruscolo, R. Najmanovich, and E. Domany, Phys. Rev. Lett. **82**, 656 (1999).
[86] L. D. Landau and E. M. Lifshitz, *Statistical Physics*, 3rd ed. (Pergamon, Oxford, 1980).
[87] S. S. Plotkin, J. Wang, and P. G. Wolynes, Phys. Rev. E **53**, 6271 (1996).
[88] V. S. Pande, A. Y. Grosberg, and T. Tanaka, Folding Des. **2**, 109 (1997).
[89] A. Fernández, K. S. Kostov, and R. S. Berry, J. Chem. Phys. **112**, 5223 (2000).
[90] This term contains in principle a resummation of all the moments of a virial expansion of the entropy $S_V(\{Q_i^f\}|\{Q_i^o\})=\Sigma_i s_i^o\times(Q_i^f-Q_i^o)+\Sigma_{i,j}s_{i,j}^o\times(Q_i^f-Q_i^o)\times(Q_j^f-Q_j^o)+\cdots$, which is a slowly convergent expansion consisting of two-body, four-body, and higher-order terms.
[91] P. J. Flory, J. Am. Chem. Soc. **78**, 5222 (1956).
[92] A. Gutin and E. Shakhnovich, J. Chem. Phys. **100**, 5290 (1994).
[93] A. V. Finkelstein and A. Y. Badretdinov, Mol. Biol. **31**, 391 (1997).
[94] I. N. Berezovsky, A. Y. Grosberg, and E. N. Trifonov, FEBS Lett. **466**, 283 (2000).
[95] H. S. Chan and K. A. Dill, J. Chem. Phys. **92**, 3118 (1990).
[96] K. A. Dill, K. M. Fiebig, and H. S. Chan, Proc. Natl. Acad. Sci. U.S.A. **90**, 1942 (1993).
[97] As an analogous example, 20 tosses of a fair coin have a larger combinatorial entropy than 10 tosses of a coin biased to heads, plus 10 more tosses of coin equally biased to tails, even though the average in both cases (the analogue to $Q$) is 10 heads.
[98] M.-H. Hao and H. A. Scheraga, J. Phys. Chem. **98**, 4940 (1994).
[99] We could equivalently have explicitly invoked this by introducing the Lagrange constraint $\Sigma_i Q_i=MQ$ into the problem from the outset.
[100] L. S. Itzhaki, D. E. Otzen, and A. R. Fersht, J. Mol. Biol. **254**, 260 (1995).
[101] H. Nymeyer, N. D. Socci, and J. N. Onuchic, Proc. Natl. Acad. Sci. U.S.A. **97**, 634 (2000).
[102] Note that by the structure of Eq. (3.19), Eq. (4.14b) is satisfied for all $Q$, i.e., when the energies are tuned to extremize $\Delta F^{\ddagger}$, the $Q_i$ are all equal essentially for all $Q$. Thus, in the model there is full symmetry in the ordering of the protein. However, when the entropy is exactly counted, and also when the entropy cutoff mentioned after Eq. (3.28) is present, $Q_i(Q)=Q$ only at the barrier peak.
[103] B. Derrida, Phys. Rev. B **24**, 2613 (1981).
[104] Averaging over native disorder in calculating $\overline{Q_i}$ leaves the residual dependence on loop entropy for each contact probability, which is then summed using $\Sigma_i\overline{Q_i}=MQ$.
[105] The variables parametrizing the model are $(N,z,\overline{E}/zN,\overline{\epsilon},s_o,b,\alpha)=(27,28/27,0,-3,1.35,0,0.9)$. The loop length distribution for the 28 loops in the native structure of Fig. 1 is $\{3(\times5),5(\times4),7(\times6),9(\times6),11(\times2),13,21,23(\times3)\}$. The mean of the distribution is $\overline{l}\cong9.14$. See Refs. 49, and 52 for a more complete description.
[106] C. Levinthal, in *Mossbauer Spectroscopy in Biological Systems*, edited by P. DeBrunner, J. Tsibris, and E. Munck (University of Illinois Press, Urbana, IL, 1969), pp. 22–24.
[107] S. S. Plotkin and P. G. Wolynes, Phys. Rev. Lett. **80**, 5015 (1998).
[108] Z. Guo and D. Thirumalai, Biopolymers **36**, 83 (1995).
[109] The reduction in conformational entropy at low $Q$ due to the elimination of conformations which happen to have residues in proximity (Ref. 87) is not included here because it is a smaller effect than the other contributions to the entropy.
[110] A. R. Viguera, V. Villegas, F. X. Aviles, and L. Serrano, Folding Des. **2**, 23 (1996).
[111] D. E. Kim, C. Fisher, and D. Baker, J. Mol. Biol. **298**, 971 (2000).
[112] V. Munoz and L. Serrano, Folding Des. **1**, R71 (1996).
[113] S. J. Hagen, J. A. Hofrichter, A. Szabo, and W. A. Eaton, Proc. Natl. Acad. Sci. U.S.A. **93**, 11615 (1996).
[114] B. M. Brown and R. T. Sauer, Proc. Natl. Acad. Sci. U.S.A. **96**, 1983 (1999).
[115] M. O. Lindberg, J. Tangrot, D. E. Otzen, D. A. Dolgikh, A. V. Finkelstein, and M. Oliveberg, J. Mol. Biol. **314**, 891 (2001).
[116] M. Oliveberg, Y. Tan, M. Silow, and A. Fersht, J. Mol. Biol. **277**, 933 (1998).
[117] P. G. Wolynes, Nat. Struct. Biol. **4**, 871 (1997).
[118] R. E. Burton, J. K. Myers, and T. G. Oas, Biochemistry **37**, 5337 (1998).
[119] S. S. Plotkin, Proteins: Struct., Funct., Genet. **45**, 337 (2001).